1 of 1

GENETIC PROBES OF STRUCTURE/FUNCTION RELATIONSHIPS IN THE Q_B BINDING SITE OF THE PHOTOSYNTHETIC REACTION CENTER†

Deborah K. Hanson,* David M. Tiede,‡ Sharron L. Nance, Chong-Hwan Chang, and Marianne Schiffer

Biological and Medical Research Division

‡Chemistry Division

Argonne National Laboratory

Argonne, Illinois 60439

Running title: Genetic Probes of Q_B Site Structure and Function

---

Supported by the U.S. Department of Energy, Office of Health and Environmental Research or ‡Office of Basic Energy Sciences, under Contract No. W-31-109-ENG-38. C.-H. C. and M. S. are also supported by Public Health Service Grant GM36598.

*To whom correspondence should be addressed.

ABSTRACT

In photosynthetic reaction centers, a quinone molecule, Q_B, is the terminal acceptor in light-induced electron transfer. The crystal structure of the reaction center implicates the protonatable amino acid residues L212Glu and L213Asp in the binding of Q_B to the reaction center and in proton transfer to the anionic forms of Q_B generated by electron transfer from Q_A. Here we report the construction of the double mutant L212Ala-L213Ala by site-specific mutagenesis, and the isolation and preliminary biophysical characterization of revertant and suppressor strains that have regained the ability to grow under photosynthetic conditions. Our results show that neither L212Glu nor L213Asp is essential for efficient light-induced electron or proton transfer in *Rhodobacter capsulatus* and that second-site mutations, located within the Q_B binding pocket or at a more distant site, can compensate for mutations at L212 and L213. Acquisition of a single negatively charged residue (at position L213, or on the other side of the binding pocket at position L225) or loss of a positively charged residue (at position M231) is sufficient to restore activity to the complex.

The photosynthetic reaction center (RC) from purple bacteria is the first membrane-bound protein for which an atomic structure has been determined by x-ray diffraction (Deisenhofer and Michel, 1989; Feher et al., 1989; Chang et al., 1986, 1991). The RC in the photosynthetic membrane mediates light-initiated redox chemistry, producing a transmembrane charge separation and membrane potential (reviewed in Feher et al., 1989). This protein thus provides a general model system for unraveling the fundamental mechanisms of transmembrane electron transfer.

The RC complex is composed of three protein subunits, the intermembrane L and M chains and the H polypeptide, as well as several cofactors: four bacteriochlorophylls, two bacteriopheophytins, two quinones, and one nonheme iron atom. It is well established that the cofactors are the chemically active components of the photosynthetic process (reviewed in Kirmaier and Holten, 1987). Other than its obvious architectural role, the detailed contribution of the protein to the electrochemistry of this process is more obscure. An approximate twofold symmetry relates the L and M subunits and their associated cofactors, suggesting two routes of charge separation across the photosynthetic membrane. However, the normal photochemistry follows only a single pathway, the one that is primarily associated with the L subunit. Upon light activation, an electron is transferred from the "special pair" bacteriochlorophyll dimer (P) to the L-side bacteriopheophytin. The final steps involve the transfer of electrons from the primary quinone (Q_A) to the secondary quinone (Q_B) near the cytoplasmic face of the membrane (Deisenhofer and Michel, 1989; Feher et al., 1989; Kirmaier and Holten, 1987; Michel-Beyerle et al., 1988).

Although Q_A and Q_B in the RCs of *Rhodobacter capsulatus* and *Rhodobacter sphaeroides* are chemically identical ubiquinone molecules, their binding sites and *in situ* chemical properties are quite different (Crofts and Wraight, 1983). As the primary quinone acceptor in the chain of light-induced reactions, Q_A receives a single electron from bacteriopheophytin. Q_A is not protonated and cannot be reduced further; the electron is transferred from Q_A to Q_B within 200 μsec. Q_B, however, accepts electrons from two successive light-induced turnovers of Q_A and then gains two protons from the cytoplasmic side of the membrane, forming Q_BH_2 (Crofts and Wraight, 1983; Feher et al., 1989). A "bucket brigade" mechanism involving a channel of protonatable amino acid side chains has been proposed for the transfer of protons from the cytoplasm to the Q_B anion(s), which have no contact with the aqueous environment (Allen et al., 1988; Paddock et al., 1989). The quinol form diffuses out of the RC (McPherson et al., 1990) and is replaced by a quinone from the membrane pool; Q_BH_2 is reoxidized by the cytochrome bc_1 complex.

Clearly, characteristics of the protein and cofactor structure influence both the chemical properties of the quinones and the routes of photoinitiated electron and proton transfer. Individual amino acids that break the twofold symmetry are probably responsible for the different chemical and spectral properties of the symmetrically related cofactors, and for the unidirectionality of electron transfer. In this paper, we discuss the protein residues that surround the quinone cofactors and report the construction and initial characterization of a site-specific double mutant of *R. capsulatus* that probes the function of two residues in the Q_B site which differ significantly from their equivalents in the

Q_A site. We also report the genetic and physical characterization of revertant and suppressor strains we isolated that have regained the ability to grow under photosynthetic conditions.

MATERIALS AND METHODS

Structure analysis. To characterize the quinone binding sites and identify the differences between the Q_A and Q_B sites, the *R. sphaeroides* RC structure (Chang et al., 1986; Chang et al., 1991) was examined on an Evans and Sutherland PS300 graphics terminal by using the computer program FRODO (Jones, 1978). The residue numbering of *R. capsulatus* (Youvan et al., 1984) was used for all RCs; numbers correspond to the alignments suggested by Michel et al. (1986), Belanger et al. (1988), and Ovchinnikov et al. (1988a, 1988b).

Mutant construction. The system of plasmids described by Bylina et al. (1986, 1989) was used for the construction of site-specific mutants in *R. capsulatus*. For mutagenesis, the HindIII-KpnI fragment containing the majority of the L gene (residues 1-253) was subcloned into the bifunctional vector pBS (Stratagene). Site-specific mutagenesis was performed according to the method of Kunkel et al. (1987) using a kit obtained from Bio-Rad. A 30-mer containing two single base changes that encode alanine residues at positions L212 and L213 (5′-CGGAAGTAGGTGGCCGCGTGGTCCGGCGTC-3′, complementary to the noncoding strand) was used to prime synthesis from the wild-type template. *E. coli* colonies harboring the mutant plasmids were detected by colony hybridization with the end-labeled oligonucleotide (Sambrook et al.,

1989). The presence of the mutation was confirmed by dideoxy sequencing of double-stranded DNA performed according to directions from a kit (Sequenase, United States Biochemical). The mutant L gene was returned to the *puf* operon in plasmids pU29 and pU2922 [Bylina et al. (1986) and Bylina et al. (1989), respectively]. Mutant plasmids were transferred to the *R. capsulatus* deletion strain U43 (LHI^-, $LHII^-$, RC^-; Youvan et al., 1985) by conjugation with *E. coli* donor strain S17-1 (Simon et al., 1983). *R. capsulatus* transconjugants were selected on RCV medium (Weaver et al., 1975); plates were incubated aerobically in the dark. Kanamycin (25 μg/ml) was included in all media to ensure presence of the plasmid. Single colonies of transconjugants were restreaked twice on MPYE agar (Davidson et al., 1989) for single colonies. In all cases, the "wild-type" strain is U43 complemented by plasmid pU2922.

The double mutant L212-213AA was routinely propagated under chemoheterotrophic growth conditions (semi-aerobic, dark, 34°C) to avoid the selection of photocompetent revertants; the medium was either RCV^+ (Yen and Marrs, 1977), or one that consisted of 2/3 RCV, 1/3 MPYE ("RPYE" medium). To confirm the presence of the desired mutation, the plasmid was recovered from a culture of a chemoheterotrophically-grown transconjugant and resequenced. For determinations of photosynthetic growth phenotype, MPYE agar containing kanamycin was spotted with 5 μl of strains grown chemoheterotrophically and then incubated under a light intensity of 30 W/m^2 in anaerobic jars (Gaspack systems, BBL). Growth of the mutant under photosynthetic conditions relative to that of wild-type and deletion strains was evaluated no later than 2-3 days after

inoculation in order to prevent the possible contribution of revertants to the observed phenotype.

Isolation and genetic characterization of revertants. Revertants of the L212-213AA mutant were selected under photosynthetic conditions by incubating plates spread with chemoheterotrophically-grown cultures of this strain. Typically, revertants began to appear in about one week as papillae. Both spontaneous and UV-induced PS^+ revertants were selected from plates grown under relatively high [30 W/m^2] and relatively low [20 W/m^2] illumination. Any effect of the mutagenesis or selection schemes is not apparent at this stage of the analysis. (Revertants do not necessarily represent independent mutational events, since the same culture was used as the starting material for all revertants selected.) Single colonies of revertants were purified through two subsequent rounds of photosynthetic culture of single colonies. Once the purification was completed, cultures for physical or genetic analysis were always grown chemoheterotrophically to eliminate selective pressure for additional reversion events. Plasmids recovered from chemoheterotrophic cultures of the purified revertants were conjugated into the U43 deletion strain a second time in order to determine whether the photosynthetic phenotype was cotransferred with the plasmid. The segments of the plasmid containing the L and M genes were subcloned into the pBS vector and were sequenced.

In order to define which segments of DNA were necessary and sufficient to confer the photosynthetic phenotype, combinations of revertant and wild-type L and M genes were engineered. In the plasmids pU29 and pU2922, a

HindIII-KpnI fragment contains the majority of the L gene and a KpnI-BamHI fragment contains the majority of the M gene; a HindIII-BamHI fragment thus carries both L and M. These sites, unique in pU29, were used to combine segments of the revertant and wild-type *puf* operons. Revertant L and M genes were shuttled into versions of pU29 or pU2922 bearing L or M genes that were tagged with restriction sites. In one version, an additional BalI site was generated by site-specific mutagenesis at codons L181-182; in another, a BglII site was generated at the M86 codon. Successful replacement of the wild-type segment was monitored by screening small-scale plasmid preparations for loss of the appropriate restriction site. EcoRI-SacI fragments bearing the chimeric *puf* operons were switched for the equivalent tagged fragment in the broad host range vehicle pU2922. Each of these plasmids was then transferred to *R. capsulatus* via conjugation with *E. coli* strain S17-1.
The ability of strains bearing the chimeric plasmids to grow under photosynthetic conditions was determined as described above; chemoheterotrophically-grown cultures of the strains were used as inocula, and the wild-type (U43[pU2922]), deletion (U43), and double mutant (U43[pR212AA]) strains were included as positive and negative controls for growth. Strains that grew within two days were scored positive for photosynthetic growth. During the two day incubation, no papillae (revertants) appeared in the spot that corresponded to the inoculum from the double mutant culture, and spots corresponding to strains bearing chimeric plasmids also remained uniform.

Preparation of chromatophores and reaction centers. One representative of each class of revertants/suppressors was chosen for kinetic

experiments (Class 1 -- U43[pLL4]; Class 2 -- U43[pHL4]; Class 3 -- U43[pLL7]). Chromatophores were prepared from 100 ml cultures of these strains and also from the wild-type (U43[pU2922]), and double mutant (U43[pR212AA]); all cultures were grown semi-aerobically in the dark in RPYE medium containing kanamycin. Briefly, cells were harvested, resuspended in 50 mM Tris (pH 7.8) that included small amounts of lysozyme and DNase, and disrupted by passage through a French Pressure cell. Cell debris was removed at 10,000 x g for 20 min, and chromatophores were pelleted by centrifugation at 180,000 x g for 2 hr. Crude RCs were prepared by extracting chromatophores suspended in 50 mM Tris (pH 7.8)/100 mM NaCl with 1% β-octylglucoside (Sigma Chemical Co.) for 1 hr. at 23°C. Following centrifugation at 180,000 x g in a Beckman TL-100 tabletop ultracentrifuge, the supernatants containing RCs were concentrated and washed with 10 mM Tris (pH 7.8)/0.8% β-octylglucoside by using Centricon 10 concentrators (Amicon). RCs were stored in this buffer at -70°C.

Kinetic measurements of electron transfer rates. The kinetics of recovery of the photooxidized bacteriochlorophyll dimer were monitored at 810 nm in chromatophores, diluted in 50 mM Tris (pH 7.8) to an A_{860} of 0.4-1.0 cm^{-1}. Lauryldimethylamine N-oxide (LDAO) was added to a final concentration of 0.06% to release cytochrome c_2 from the interior of the chromatophore vesicle, and to disrupt cytochrome c_1/RC complexes, which can rapidly reduce the oxidized dimer (Prince et al., 1986). Rates were also determined after the addition of 200 μM atrazine. Multiphasic kinetics were fitted with two exponentials plus a variable baseline. The baseline component (corresponding to 1-15% of the total absorption

change) was needed because a third long-lived component (several seconds) was observed in all samples, even in the presence of atrazine. The rates derived from these fits are dependent upon the model used for fitting the experimental traces. Therefore, these values should be considered preliminary. Clearly the present model will fail to associate long-lived (seconds) kinetic components with the $P^+Q_AQ_B^-$ recombination reaction. In RCs isolated from *R. sphaeroides*, Takahashi and Wraight (1990) found lifetimes (τ) of ~1 sec for the wild-type and ~10 sec for a site-specific mutant that were associated with the $P^+Q_AQ_B^-$ back reaction. Paddock et al. (1991), also using isolated *R. sphaeroides* RCs, reported a lifetime of 1.1 sec for wild-type, and lifetimes ranging from 0.2-1.1 sec for a set of mutants. We find that in *R. capsulatus* chromatophores, the long-lived (seconds time scale) components are minor and inconsistently present. At the present time, we are not considering these components to be indicative of a $P^+Q_AQ_B^-$ back reaction. Further experiments will determine the optimal fitting procedures.

The rates of electron transfer from Q_A to Q_B following a single laser flash were determined in wild-type, double mutant, revertant, and suppressor strains by comparing kinetics observed at 860 nm and 770 nm. The absorption transients at 860 nm report directly on the redox state of the dimer, while the transients at 770 nm reflect electrochromic shifts of the L-side bacteriopheophytin, which responds to the redox state of P and, differentially, to Q_A^- and Q_B^- (Vermeglio and Clayton, 1977). Chromatophores were diluted in 50 mM Tris (pH 7.8) to an A_{860} of 0.9-1.0 cm^- Kinetics at each wavelength were also determined following the addition of 200 μM atrazine to each sample. The results following 40

flashes were averaged to enhance the signal-to-noise ratio. Multiphasic kinetics at 860 nm were fitted with two exponentials; three exponentials were used to fit kinetics at 770 nm.

Cytochrome photooxidation assays. Photooxidation of cytochrome c_2 under continuous illumination at 0.6 W/cm^2 was monitored at 550 nm. Samples of reaction centers, diluted to an A_{800} of 0.2-0.4 cm^{-1} in 10 mM Tris (pH 7.8)/1 mM EDTA/0.8% β-octylglucoside, supplemented by 40 μM ubiquinone-0 (UQ_0) and 10 μM *R. capsulatus* cytochrome c_2, were subjected to continuous illumination. Rates were also measured after the addition of 300 μM atrazine. The absorbance change corresponding to one cytochrome c_2/RC was calibrated by the initial absorbance decrease at 600 nm in the sample prior to the addition of cytochrome. Dithionite-reduced horse cytochrome *c* did not consistently bind to RCs or exhibit reproducible steady-state oxidation kinetics. Instead, *R. capsulatus* cytochrome c_2 was used as the electron donor for these assays. This cytochrome binds with higher affinity, exhibits faster electron donation rates, and does not require additional reduction in aerobic solutions.

Transient Optical Absorbance Spectrometer and Curve Fitting. Transient optical absorbance changes were measured with a single beam spectrometer of local design. Probe light from a 50 Watt tungsten lamp was passed through a monochrometer, focused upon the sample, then collected and passed through a second monochrometer before being detected with an avalanche photodiode (RCA). Steady-state excitation light (0.6 watt/cm^2) was provided by a 50 watt xenon arc lamp, filtered through a 650 nm band-pass filter, and gated with an Uniblitz shutter (3 msec risetime).

Flash excitation was provided by a 20 nsec, 590 nm, 1.5 mJ/cm^2 pulse provided by a frequency-doubled YAG pumped rhodomine dye laser. The instrument was operated with a response time of 5 μsec. Optical absorbance transients were fitted as the sum of two or three exponential decays with a Marquadt non-linear least squares fitting program provided by Dr. Seth Snyder (Argonne National Laboratory). The uncertainties in the $Q_A^- Q_B \rightarrow Q_A Q_B^-$ lifetime measurements reflect the range of values that were resolved in the 770 nm transients that were not present in the 860 nm transients.

RESULTS

Structural analysis of the quinone binding sites.

i. General features. Table I lists the amino acid residues that form the surface of the cavity in which each quinone is located in the purple bacteria *Rhodopseudomonas viridis* (Michel et al., 1986), *R. sphaeroides* (Williams et al., 1983, 1984), *R. capsulatus* (Youvan et al., 1984), and *Rhodospirillum rubrum* (Belanger et al., 1988), and the green bacterium *Chloroflexus aurantiacus* (Ovchinnikov et al., 1988a,b).

Homologous residues from the D, DE, and E helices (Deisenhofer and Michel, 1989; Feher et al., 1989; Chang et al., 1991; El-Kabbani et al., 1991) of the L and M chains define both quinone binding sites. The Q_A site is formed by residues of the M chain. The Q_B site consists primarily of residues from the L chain, but amino acids from both the M and H chains are also nearby. The addition of seven more M-chain residues between the D and DE helical segments, near the local twofold axis, breaks the symmetry between the L and M chains in this region of

the molecule. Glutamic acid M232 in the middle of this segment provides the fifth and sixth ligands to the Fe atom.

The interface of the H subunit with the L and M subunits is remarkable for the large number of charged groups within it. These groups may be important for the function of the RC, possibly in proton transfer to Q_B, because they are more numerous than those observed in interfaces of multisubunit proteins in general. The residues around the quinone sites not only influence quinone binding and function but also contribute to the global charge distribution in the reaction center molecule; therefore, they might have an indirect influence on electrochemistry at a distant point, such as at the special pair.

ii. Residues that form the Q_A site. It is remarkable that 12 residues of the 18 that define the Q_A site are conserved in all five organisms (Table I). The largest number of substitutions is found in *R. viridis*, where the replacements are alanine for methionine at M216, isoleucine for methionine at M254 and M260, and valine for isoleucine at M263. These substitutions replace a large hydrophobic residue with a smaller one, thereby increasing the volume of the binding pocket by 110 $Å^3$ in this species compared to that of the other purple bacteria. In *R. viridis* and *C. aurantiacus*, the quinone in the Q_A site is a menaquinone, while it is a ubiquinone in the other three RCs, which share identical Q_A sites. Only five of the residues forming the Q_A site are polar: threonines M220 and M259, asparagine M257, and histidines M217 and M263 that are iron ligands; all are conserved in the four species of purple bacteria.

iii. Residues that form the Q_B site. Of the L-chain residues that form the Q_B site, only nine out of 19 are conserved. These residues are histidines L190 and L230 (iron ligands), glutamic acid L212, tyrosine L222, serine L223, glycine L225, leucine L193, and phenylalanine L216. Five of these conserved residues are charged or polar, while only three are hydrophobic. Histidine L190 and serine L223 form hydrogen bonds with the carbonyl oxygen atoms of the quinone (El-Kabbani et al., 1991; Allen et al., 1988; Deisenhofer and Michel, 1989). At five positions in the Q_B site (L186, L194, L224, L229, and L232), conservative substitution of one aliphatic hydrophobic residue for another occurs. At three of these positions (L194, L224, and L229), the β-forked residues isoleucine and valine are found and thus might be required for function.

R. viridis is the only species in which a nonpolar residue (alanine) is found at L226. At position L215, an aromatic residue is conserved, but it can be either polar (tyrosine) or nonpolar (phenylalanine). At position L213, both asparagine (polar but not charged at neutral pH) and aspartic acid (charged) occur. Glutamic acid M232 forms part of the Q_B binding site; this residue has no equivalent in the L chain. The Q_B site is occupied by ubiquinones in all but *C. aurantiacus*, where it is a menaquinone.

iv. Comparison of the Q_A and Q_B sites. Three residues (L186, L220, and L232) in the Q_B site and three residues (M213, M254, and M266) in the Q_A site (see Table I) are near the phytyl tails. These residues in the Q_B site are smaller than the ones in the Q_A site in most of the organisms, resulting in the enlargement of the entrance to the Q_B site which may

facilitate the exchange of Q_B with the quinone pool. No exchange of Q_A is observed *in vivo;* to exchange Q_A *in vitro,* a breathing motion of the protein is required. The phytyl tail of Q_A extends through a narrow channel that appears to be too small for the head group to move through. The channel is also constricted by a conserved tryptophan residue, M266, that is replaced by a smaller aliphatic residue (leucine or valine L232) in the Q_B site.

The Q_B site is significantly more polar than the Q_A site in all organisms, a difference which is reflected in the characters of the symmetry-related residues that comprise each site. Q_A site residues M246 and M247 are conserved hydrophobic alanines in all but *C. aurantiacus,* while the equivalent residues in the Q_B site at L212 and L213 are always either acidic or polar (L212, glutamic acid; L213, aspartic acid or asparagine). On the other hand, the polar residues M220Thr and M259Thr are conserved in the Q_A site, yet the equivalent residues in the Q_B site are a conserved hydrophobic leucine (L193) or glycine (L225), respectively. M256Phe is conserved in the Q_A site; the symmetry-related residue in the Q_B site is a polar tyrosine (L222). The residue at M260 is always hydrophobic, and the equivalent residue at L226 in the Q_B site is usually polar.

Not listed in Table I is glutamic acid residue H175 which forms the bottom of the Q_B cavity on the cytoplasmic side. H175Glu is part of a circular patch of charged residues that forms the interface between the L, M, and H subunits (Chang et al., 1991). The center of this region is located below the Q_B site; the patch extends to the Q_A site.

Interestingly, aspartic acid L213 and glutamic acid residues H175 and L212 do not appear to participate in salt bridge formation.

Double mutant L212Glu-L213Asp → L212Ala-L213Ala. The most striking difference in the charge distribution at the two quinone sites is caused by the presence of two acidic residues L212Glu and L213Asp in the Q_B site (see Figure 1A). In order to probe the function of these residues in both electron and proton transfer, we constructed a double mutant of *R. capsulatus* (L212-213AA, Figure 1B) in which the glutamic and aspartic acid residues at L212-213 were replaced by alanine residues (which are found at the equivalent positions in the Q_A site). This mutant does not grow under photosynthetic (anaerobic, light) conditions. However, optical spectra of suspensions of cells grown chemoheterotrophically (semi-aerobic, dark) showed absorptions at 875 nm and near 800 nm that are characteristic of normal amounts of properly assembled light-harvesting I and RC complexes. EPR spectra performed with chemoheterotrophically-grown cells and isolated RCs showed a triplet state of the bacteriochlorophyll dimer that displays wild-type characteristics (not shown; M. C. Thurnauer, R. Rustandi, T. Perkins, and C. Wu, unpublished observations). Also, the time constant of the stimulated emission decay of the singlet excited state of the dimer is similar to that observed for wild-type strains (Chan et al., 1991). These data show that the double mutation does not interfere with assembly of the RC nor its function in primary charge separation events. Therefore, it is likely that replacing these acidic residues with alanines has impaired RC function by altering the affinity of the site for ubiquinone, changing the redox potential of bound Q_B, and/or

preventing the formation of Q_BH_2 by interfering with the proton transfer step. Additional characteristics of its phenotype are discussed below.

Isolation of revertants and suppressors of the L212-213 double mutation. By incubating plates under photosynthetic conditions, revertants of the plasmid-borne L212-213AA mutant were selected. Plasmids were recovered from the photosynthetically competent strains and the L and M genes were sequenced. To date, sequence data have delineated at least five classes of revertants and suppressors (Table II), and we discuss the genetic and biophysical characterization of Classes 1-3 in detail below. In members of Classes 4 and 5, initial genetic characterization has revealed no changes in the sequenced regions; the original L212-213 double mutation is still present. The suppressor mutation is plasmid-borne in Class 4 and is chromosomal in Class 5. None of the reversion events restored a polar residue at position L212. In fact, our results show that there is no absolute requirement for polar residues at either L212 or L213.

Genetic Characterization of Revertants and Suppressors

i. Classes 1 and 2. Only two of the 24 photosynthetically competent strains characterized so far carry a reversion at one of the original sites and in both, L213Ala has reverted through a transversion (GCC → GAC) to the wild-type aspartic acid residue (Class 1, Table II; Figure 1C). No other sequence changes were found.

The second class of photosynthetically competent strains retains the original double mutation at L212-213 and carries a third mutation at position L225 that acts as an intragenic suppressor of the double

mutation. This amino acid, normally a glycine residue that is a part of the loop before the E helix and is conserved in the above five species, has been changed by a transition to an aspartic acid residue (GGC → GAC). It is located on the opposite side of the Q_B binding pocket from L213. Molecular modeling of the L225Gly → Asp substitution using the *R. sphaeroides* RC structure showed that L225Asp could point towards Q_B, its oxygen atoms occupying essentially the same space as those of L213Asp (Fig. 1D). No other changes were found in the sequenced region.

In order to test whether the mutation observed in each class of revertant was sufficient to restore the photosynthetic phenotype when present in concert with the remaining site-specific mutations, we engineered combinations of revertant and wild-type genes of the *puf* operon. For Class 1 and Class 2 strains, the L gene carrying the mutations described above was sufficient to confer the photosynthetic phenotype when coupled with a wild-type M gene. Since photosynthetic competence is a plasmid-borne trait in both classes (Table II), the possibility of finding compensatory mutations in the H gene is also eliminated, and the mutations described can be directly correlated with the restoration of the ability to grow under photosynthetic conditions.

ii. Class 3. Sequence analysis, coupled with a complementation test, has shown that the representatives of Class 3 carry a mutation in the M chain that acts as an intergenic suppressor of the L212-213AA double mutant phenotype. In these strains (which retain the original double mutation at L212-213), amino acid M231, normally an arginine residue that is involved in conserved ion pair interactions with H125Glu and H232Glu

(Figure 2A; Chang et al., 1991) has been changed by a transversion to a leucine residue (CGC → CTC; amino acid substitution modeled in Figure 2B). No other sequence changes were found in the L or M genes of the plasmid recovered from these strains. Plasmid constructions that coupled the L gene from these strains (which carries the double mutation L212Ala-L213Ala) with the wild-type M gene did not confer the photosynthetic phenotype upon transfer of the chimeric plasmid to the *R. capsulatus* deletion strain. When both the L and M genes isolated from these strains were combined with the remainder of the wild-type plasmid, cotransfer of the photosynthetic phenotype with the plasmid was observed. These results confirm that the sequence alteration in the M gene of the revertant plasmid compensates for the L212-213AA double mutation still present in the L gene of these strains.

Reaction Center Photochemistry

a. Charge Recombination Rate. The rates of recovery of the photooxidized dimer in LDAO-treated chromatophore preparations of wild-type, double mutant, revertant, and suppressor strains were measured by monitoring the absorbance change at 810 nm following a single laser flash (590 nm). Multiphasic decay kinetics were observed. Table III shows the best fits obtained with two exponentials and a seconds time scale baseline component. With this fitting procedure, a consistent set of kinetic parameters could be extracted and assigned, although other kinetic models are possible (see Materials and Methods). Recombination from the $P^+Q_A^-Q_B$ or $P^+Q_AQ_B^-$ state was associated with the faster or slower exponential, respectively.

In the wild-type, the fast component of 60 msec represented about 40% of the total absorbance change. The addition of 200 μM atrazine, a competitive inhibitor of Q_B binding, was found to increase the extent of this fast component to 75%, and the rate increased to a τ (=1/k) of 40 msec. Correspondingly, the addition of atrazine caused the amplitude of the slower component to diminish substantially to 25%. The atrazine sensitivity of the slow component identifies it as being due to recombination from $P^+Q_AQ_B^-$. In contrast, the relative extents of the fast and slow components in the photosynthetically incompetent double mutant were not discernably changed by the addition of atrazine. The absence of an appreciable atrazine effect in the double mutant suggests that either $Q_A \rightarrow Q_B$ electron transfer has been blocked or that atrazine does not bind effectively. The majority of the charge recombination in this strain displays fast kinetics, indicating that it occurs primarily from Q_A. The significance of the minor, slow (0.3 sec) decay component is not clear. It could represent heterogeneity in the Q_A recombination rates, or the existence of incomplete electron transfer from Q_A to Q_B in chromatophore membranes.

In each of the photosynthetically competent revertant and suppressor strains, an effect of atrazine on the decay kinetics was observed. In the absence of atrazine, about 30% of the absorbance change is due to the fast phase in all of these strains. As was seen in the wild-type membranes, the addition of atrazine decreases the relative extent of the slow component. Class 2 strains show the least sensitivity to atrazine in all kinetic experiments and in photosynthetic growth assays. In fact, all of the revertant and suppressor strains are more resistant to

atrazine than the wild-type in growth assays (100 μM, not shown). In the Class 3 suppressor, both the rate of the slow component and its proportion of the total absorbance change most closely resemble those of the wild-type. Again, the atrazine-sensitivity of the charge recombination kinetics indicates that electron transfer to Q_B occurs in all of the revertant and suppressor strains. These findings, and the diminished $Q_A \rightarrow Q_B$ electron transfer in the double mutant, are corroborated by measurements of electron transfer rates at 770 nm and steady-state cytochrome turnover kinetics (see below).

The identification of decay rates from $P^+Q_A^-Q_B$ and $P^+Q_AQ_B^-$ states provides a means for deriving the redox potential difference between the Q_A^- and Q_B^- states (Paddock et al., 1991; Takahashi and Wraight, 1990). If the rates obtained from our preliminary experiments (Table III) are taken at face value, the ratio of the wild-type rates predicts a ΔG of -67 mV between Q_B and Q_A, which is consistent with the value obtained from similar measurements in RCs of *R. sphaeroides* (Paddock et al., 1991; Takahashi and Wraight, 1990). Values for ΔG between Q_B and Q_A in the double mutant, Class 1, 2, and 3 strains can be calculated to be -52, -30, -36, and -75 mV, respectively. The differences between these values and that of the wild-type is smaller than those derived from studies of isolated RCs from mutants of *R. sphaeroides* (Paddock et al., 1991; Takahashi and Wraight, 1990).

b. Steady-State Cytochrome Photooxidation

The steady-state rate of photooxidation of ferrocytochrome c_2 by RCs was monitored at 550 nm. This assay provides a measure of the efficiency of

cyclic turnover of Q_B by the reaction center (Paddock et al., 1988). Multiple rapid cytochrome turnovers were observed in wild-type RCs (Figure 3A), indicating rapid equilibration of Q_BH_2 with the quinone pool. In the presence of 300 μM atrazine, which blocks electron transfer beyond Q_A, only one rapid turnover was observed. Atrazine has no effect on the turnover kinetics of RCs from the double mutant (Figure 3B). The rapid oxidation of approximately one cytochrome c_2/RC was observed both in the presence and absence of atrazine, indicating that the replacement of the glutamic and aspartic acid residues by alanines in the double mutant strain prevents multiple turnovers of Q_B. This conclusion is also supported by the charge recombination kinetics (described above) in this mutant.

Reaction centers isolated from the Class 1 revertant and Class 3 suppressor strains are capable of multiple turnovers of cytochrome c_2 (Figures 3C and 3E, respectively). This observation serves as independent confirmation, apart from the photosynthetic growth assay, that RCs carrying the sequence changes described above are photochemically active. The initial turnover rate is similar to that of the wild-type, but at longer times, the rate becomes slower. A single fast turnover was also observed in RCs from the Class 2 suppressor strain, but the secondary turnover rate is especially slow (Figure 3D). In spite of this apparent limitation, the extent of photosynthetic growth of Class 2 strains under the conditions described above is comparable to that of the wild-type. The slow phase in the Class 2 suppressor strain is at least partially atrazine-sensitive, indicating that although secondary cytochrome turnovers are slow, they still occur through

multiple turnovers of Q_B. The experiments described below show that transfer of the first electron from Q_A to Q_B is not dramatically affected in this strain. At present, we cannot explain why cytochrome (or Q_B) turnover is slow in Class 2 RCs. It is possible that transfer of the second electron or proton transfer is rate-limiting under these experimental conditions, or that the Q_B site is not fully occupied. However, the addition of excess UQ_0 did not affect the turnover rate. Experiments to determine the pH dependence of this reaction and the rate of transfer of the second electron to Q_B are in progress.

c. Kinetics of electron transfer from Q_A to Q_B

The rate of electron transfer from Q_A to Q_B following a single flash was determined in chromatophores by comparing the kinetics of the photoinduced electrochromic shift of the L-side bacteriopheophytin, observed at 770 nm, to the kinetics resulting from bacteriochlorophyll dimer photochemistry monitored at 860 nm (Figure 4). The additional fast component that is present in the 770 nm kinetics has been attributed to photochemical electron transfer between the quinones (Vermeglio and Clayton, 1977). In wild-type chromatophores, the decay of the additional fast component was found to have a lifetime (τ) of 55 ($\pm$ 15) μsec; this component represented 17% of the absorbance change at 770 nm (Figure 5A, Table IV). The relative contributions of Q^- and P^+ to the bacteriopheophytin absorption changes are wavelength dependent; in reaction centers from *R. sphaeroides* the proportion of the absorbance decay at 770 nm due to $Q_A \rightarrow Q_B$ transfer is greater, about 28% (Vermeglio and Clayton, 1977). We did not attempt to determine the wavelength

optimal for Q^- contributions in these initial characterization experiments.

When atrazine was added to the sample of wild-type chromatophores, the contribution of the fast phase to the total absorbance change dropped from 17% to 5% (Table IV, Figure 5A), indicating that the majority of the fast component was due to the transfer of an electron from Q_A to Q_B. The presence of a residual fast kinetic component in the 770 nm transients agrees with the residual slow phase that remains in the recombination kinetics (described above; Table III). These samples were not scrupulously dark-adapted, therefore this component could arise from RCs which retained a long-lived Q_B^- state since inhibitors only compete effectively with fully oxidized or reduced forms of Q_B (Wraight and Stein, 1980; Vermeglio et al., 1980).

The double mutant does show a small, atrazine-insensitive rapid decay of the 770 nm absorption change (Figure 5B, Table IV), which correlates with the presence of a slow, atrazine-insensitive phase in the charge recombination kinetics (Table III). These kinetic components could reflect the presence of a partial $Q_A \rightarrow Q_B$ electron transfer reaction in this strain.

The kinetics at 770 nm in the photosynthetically competent Class 1, 2, and 3 strains all contain a fast component that is atrazine sensitive (Figures 5C, 5D, and 5E; Table IV), which indicates that the $Q_A^-Q_B \rightarrow Q_AQ_B^-$ reaction occurs on a μsec time scale. The rate of electron transfer from Q_A to Q_B in Class 1 and 3 strains is roughly equivalent to that of the

wild-type. However, in Class 3 suppressors, this component represents only about half as much of the total absorbance change as the fast phase in the wild-type strain. It is not yet clear whether this twofold decrease in the extent of the absorbance change is meaningful. Since all of these revertant and suppressor strains carry mutations that change the electrostatic environment in this region of the RC, it is possible that the magnitude of the bacteriopheophytin electrochromic shift has changed such that the amplitude of the absorbance change at 770 nm is no longer comparable to that seen in the wild-type strain.

In Class 2 suppressors, the rate of transfer of the first electron is about two times slower than that of the wild-type, but is still too rapid to account for the observation that only one cytochrome/RC is oxidized rapidly in this strain. Results for Class 2 suppressors, and also the double mutant, include the apparently contradictory observations that some fast Q_A to Q_B electron transfer occurs while only a single cytochrome is seen to be oxidized rapidly under steady-state conditions. The most likely explanation is that the rapid formation of the $Q_A^-Q_B^-$ state is prevented under these assay conditions, possibly because the mutations interfere with the rapid uptake of a proton after transfer of the first electron to Q_B. The atrazine sensitivity of the slow cytochrome turnover in Class 2 strains indicates that multiple Q_B turnovers do occur slowly, which may imply that uptake of this first proton is the rate-limiting step in electron transfer in this strain. In the double mutant, if some electron transfer from Q_A to Q_B does occur, the photosynthetically incompetent growth phenotype and the absence of multiple cytochrome turnovers indicates that multiple electron transfer

into the quinone acceptors, i.e., the $Q_A^-Q_B^-$ state, cannot occur, possibly because proton transfer is completely blocked. Experiments to determine the rates of proton transfer in all of these strains are in progress.

DISCUSSION

Maroti and Wraight (1990) have proposed models for the sequence of photoinduced protonation steps at the Q_B site. They and Paddock et al. (1990b) suggest that the primary proton donors to the Q_B anion(s) are residues L223Ser and L190His which are within hydrogen-bonding distance of the quinone. These residues, which are not in contact with the cytosol, are thought to be replenished through a network of proton donors that connect the Q_B site in the interior of the protein with the aqueous environment. This multi-component pathway(s) for internal proton transfer -- the "bucket brigade" -- has not yet been established.

Double mutant L212Glu-L213Asp → L212Ala-L213Ala

The position of the protonatable amino acid residues L212Glu and L213Asp in the crystal structure of the RC suggests that they could contribute to the redox properties of Q_B and/or be members of the pathway for the transfer of protons to the Q_B anions. By replacing the acidic amino acids at these sites with alanines found at the symmetry-related positions in the Q_A site, we generated a photosynthetically incompetent strain of *R. capsulatus* (L212-213AA) in which successive electron transfers from Q_A to Q_B are blocked. At most, the yield of the Q_B^- state after a single flash is 30%. This deficiency could be due to a change in the redox properties of Q_B, resulting in either unfavorable thermodynamic

properties of electron or proton transfer, or an unfavorable structure that interferes with Q_B binding. We have not investigated whether quinone is bound at the Q_B site in chromatophores of the double mutant; however, the amino acid sequence at this site is the same as that found in the photosynthetically competent Class 3 suppressor strain. In separate studies from two other laboratories, site-specific mutagenesis was used to replace acidic amino acids at L212 or L213 with the amide forms in RCs of *R. sphaeroides* (Paddock et al., 1989; Takahashi and Wraight, 1990, respectively). These individual substitutions also produced photosynthetically incompetent strains, and have shown that L212Glu and L213Asp are two components of the proton transfer pathway(s) that operates in wild-type *R. sphaeroides.*

Compensation for loss of L212Glu and L213Asp in revertant and suppressor strains.

Following prolonged incubation of the *R. capsulatus* double mutant strain under photosynthetic conditions, several strains were isolated which had regained the proficiency for photoheterotrophic growth. However, sequence analysis has shown that all of the classes of revertant and suppressor strains reported here lack a protonatable residue at L212 because they retain the L212Glu → Ala mutation. Complementation tests have determined that the sequence changes observed in Class 1, 2, and 3 strains are responsible for restoration of the photosynthetic phenotype. The growth assays are corroborated by preliminary biophysical characterization (performed on preparations from dark grown cultures), which has shown that RCs bearing these sequence changes are photochemically active.

We conclude that in *R. capsulatus*, neither L212Glu nor L213Asp is absolutely required for the proton transfer pathway since a wild-type phenotype (growth within two days under photosynthetic conditions) is observed in revertant strains which couple a nonprotonatable, nonpolarizable alanine residue at L212 with a protonatable aspartic acid residue at either L213 or L225 (Class 1, L212Ala-L213Asp; Class 2, L212Ala-L213Ala-L225Asp, respectively). These results show that reacquisition of one of the two protonatable residues lost in the Q_B site of the L212-213AA mutant is one way of restoring RC activity, and that this protonatable residue can be located at a second site in the Q_B binding cavity. The lack of a requirement for an acidic residue at L212 is also shown by the substitution of lysine at this position in a herbicide-resistant mutant of *R. viridis* (Michel et al., 1990).

In RCs of Class 3 suppressor strains, compensation for the loss of negatively charged residues at L212 and L213 is achieved when a positively charged residue is lost (Arg → Leu) rather than by the addition of a negatively charged one (as seen in Class 1 and Class 2 events). However, the disruption of the ionic interactions of M231Arg with H125Glu and H232Glu (Figure 2b) essentially adds a potential negative charge by freeing the acidic residues for participation in other interactions. Also, the charge distribution of the RC has been altered. Without further kinetic and spectroscopic data, it is difficult to speculate any further about the mechanism by which suppression is actually achieved in RCs of Class 3 strains. The amino acid sequence within the Q_B binding site is identical to that of the photosynthetically incompetent double mutant. The protonatable residues H125Glu and H232Glu

are distant from L190His (about 14 Å and 18 Å, respectively), L223Ser (about 16 Å and 20 Å, respectively), and Q_B (about 14 Å and 18 Å, respectively). Direct interaction of H125Glu and H232Glu with Q_B, L223Ser, or L190His could not be achieved unless a gross structural rearrangement has occurred as a result of replacing arginine at M231 with leucine. However, this substitution does not change the structure of the RC in a way that affects transfer of the first electron from Q_A to Q_B, since the rate is comparable to that of wild-type RCs. M231Arg is not a part of either of the two proton transfer pathways proposed by Allen et al. (1988), nor are H125Glu or H232Glu.

The dramatic difference in the observed phenotypes of the *R. sphaeroides* mutant constructed by Paddock et al. (1989) (L212Gln-L213Asp; photosynthetically incompetent) and Class 1 revertants of *R. capsulatus* (L212Ala-L213Asp; photosynthetically competent) might be due to sequence or structural differences in RCs of the two organisms. However, the L-, M-, and H-chain components of the Q_B binding site of *R. capsulatus* are largely conserved in *R. sphaeroides* (see above and Table I). Of the four exceptions, three substitute one uncharged aliphatic residue for another; in the fourth, a phenylalanine residue in *R. sphaeroides* corresponds to a polarizable tyrosine residue at L215 in *R. capsulatus*. When its position in the Q_B site was modeled with the *R. sphaeroides* structure, this tyrosine residue was not within hydrogen-bonding distance of Q_B, L223Ser, or L190His. At present, the reasons underlying the different phenotypes of strains with such similar sequences are not obvious.

The replacement of M231Arg with a leucine (Class 3) at a site outside of the Q_B binding pocket shows that distant amino acid substitutions can also compensate for loss of charged groups in the Q_B site. These results indicate that there can be multiple pathways for the transfer of protons to reduced Q_B. Revertants and suppressors might use pathways different from the one used by the wild-type or the mechanism for Q_B protonation may have changed due to the alteration in the charge distribution of the RC. Clearly, existing models cannot explain the observations reported here.

Historically, protein-quinone interactions at the Q_B site have been probed by the selection and analysis of spontaneous herbicide-resistant mutants in bacteria, algae, and plants. No other mutations at L225Gly or M231Arg have been reported, even among herbicide-resistant strains. These sites are not ones likely to have been chosen for site-specific mutagenesis. Molecular modeling using the *R. sphaeroides* RC structure suggests that a single mutation of L225Gly to Asp in otherwise wild-type RCs would place two negatively charged side chains (L213Asp and L225Asp) in such proximity that these mutant RCs might not assemble. Therefore, the analysis of spontaneous suppressor mutations at L225 and M231 that compensate for the site-specific mutations at L212-213 will give us insight into the electrochemistry at the Q_B site that could not necessarily be derived from the study of spontaneous or site-specific mutations alone.

Acknowledgments: We thank D. C. Youvan for the generous gift of the *R. capsulatus* deletion strain and plasmids pU29 and pU2922, and C. Wu for

performing initial charge recombination and cytochrome turnover experiments. We also thank F. J. Stevens, M. C. Thurnauer, and J. R. Norris for helpful discussions and critical reviews of the manuscript.

REFERENCES

Allen, J. P., Feher, G., Yeates, T. O., Komiya, H., and Rees, D. C. (1988) *Proc. Nat. Acad. Sci. U.S.A. 85*, 8487-8491.

Belanger, G., Berard, J., Corriveau, P., and Gingras, G. (1988) *J. Biol. Chem. 263*, 7632-7638.

Bylina, E. J., Ismail, S., and Youvan, D. C. (1986) *Plasmid 16*, 175-181.

Bylina, E. J., Jovine, R. V. M., and Youvan, D. C. (1989) *Bio/Technology 7*, 69-74.

Chan, C-K., Chen, L. X-Q., DiMagno, T. J., Hanson, D. K., Nance, S. L., Schiffer, M., Norris, J. R., and Fleming, G. R. (1991) *Chem. Phys. Lett. 176*, 366-372.

Chang, C-H., El-Kabbani, O., Tiede, D., Norris, R., and Schiffer, M. (1991), *Biochemistry*, in press.

Chang, C-H., Tiede, D., Tang, J., Smith, U., Norris, J., and Schiffer, M. (1986) *FEBS Lett. 205*, 82-86.

Crofts, A. R., and Wraight, C. A. (1983) *Biochim. Biophys. Acta 726,* 149-185.

Davidson, E., Prince, R. C., Haith, C. E., and Daldal, F. *J. Bact. 171,* 6059-6068 (1989).

Deisenhofer, J., and Michel, H. (1989) *Science 245,* 1463-1473.

El-Kabbani, O., Chang, C-H., Tiede, D., Norris, J., and Schiffer, M. (1991), *Biochemistry,* in press.

Feher, G., Allen, J. P., Okamura, M. Y., and Rees, D. C. (1989) *Nature 339,* 111-116.

Jones, T. A. (1978) *J. Appl. Crystallogr. 11,* 268.

Kirmaier, C., and Holten, D. (1987) *Photosyn. Res. 13,* 225-260.

Kunkel, T. A., Roberts, J. D., and Zakour, R. A. (1987) *Methods in Enzymol. 154,* 367-382.

Maroti, P., and Wraight, C. A. (1990) in *Current Research in Photosynthesis,* (Baltscheffsky, M., ed.), Vol. 1, pp. 1.165-1.168.

McPherson, P. H., Okamura, M. Y., and Feher, G. (1990) *Biochim. Biophys. Acta 1016,* 289-292.

Michel-Beyerle, M. E., Plato, M., Deisenhofer, J., Michel, H., Bixon, M., and Jortner, J. (1988) *Biochim. Biophys. Acta 932*, 52-70.

Michel, H., Weyer, K. A., Gruenberg, H., Dunger, I., Oesterhelt, D., and Lottspeich, F. (1986) *EMBO J. 5*, 1149-1158.

Michel, H., Sinning, I., Koepke, J., Ewald, G., and Fritzsch, G. (1990) *Biochim. Biophys. Acta 1018*, 115-118.

Ovchinnikov, Y. A., Abdulaev, N. G., Zolotarev, A. S., Shmukler, B. E., Zargarov, A. A., Kutuzov, M. A., Telezhinskaya, I. N., and Levina, N. B. (1988a) *FEBS Lett. 231*, 237-242.

Ovchinnikov, Y. A., Abdulaev, N. G., Shmuckler, B. E., Zargarov, A. A., Kutuzov, M. A., Telezhinskaya, I. N., Levina, N. B., and Zolotarev, A. S. (1988b) *FEBS Lett. 232*, 364-368.

Paddock, M. J., Rongey, S. H., Abresch, E. C., Feher, G., and Okamura, M. Y. (1988) *Photosyn. Res. 17*, 75-96.

Paddock, M. L., Rongey, S. H., Feher, G., and Okamura, M. Y. (1989) *Proc. Nat. Acad. Sci. U.S.A. 86*, 6602-6606.

Paddock, M. L., Feher, G., and Okamura, M. Y. (1990a) *Biophys. J. 57*, 569a.

Paddock, M. L., McPherson, P. H., Feher, G., and Okamura, M. Y. (1990b) *Proc. Nat. Acad. Sci. U.S.A. 87,* 6803-6807.

Paddock, M. L., Feher, G., and Okamura, M. Y. (1991) *Photosyn. Res. 27,* 109-119.

Prince, R. C., Davidson, E., Haith, C. E., and Daldal, F. (1986) *Biochemistry 25,* 5208-5214.

Sambrook, J., Fritsch, E. F., and Maniatis, T. (1989) *Molecular Cloning: A Laboratory Manual,* Cold Spring Harbor Press, (New York).

Simon, R., Priefer, U., and Puhler, A. (1983) *Bio/Technology 1,* 37-45.

Vermeglio, A., and Clayton, R. K. (1977) *Biochim. Biophys. Acta 461,* 159-165.

Vermeglio, A., Martinet, T., and Clayton, R. A. (1980) *Proc. Nat. Acad. Sci. U.S.A.* 77, 1809-1813.

Weaver, P. F., Wall, J. D., and Gest, H. (1975) *Arch. Microbiol. 105,* 207-216.

Williams, J. C., Steiner, L. A., Ogden, R. C., Simon, M. I., and Feher, G. (1983) *Proc. Natl. Acad. Sci. U.S.A. 80,* 6505-6509.

Williams, J. C., Steiner, L. A., Feher, G., and Simon, M. I. (1984) *Proc. Natl. Acad. Sci. U.S.A. 81,* 7303-7307.

Wraight, C. A., and Stein, R. R. (1980) *FEBS Lett. 113,* 73-77.

Yen, H.-C. and Marrs, B. (1977) *Arch. Biochim. Biophys. 181,* 411-418.

Youvan, D. C., Bylina, E. J., Alberti, M., Begusch, H., and Hearst, J. E. (1984) *Cell 37,* 949-957.

Youvan, D. C., Ismail, S., and Bylina, E. J. (1985) *Gene 38,* 19-30.

FIGURE LEGENDS

FIGURE 1: Molecular model, using the *R. sphaeroides* structure, of interactions in the Q_B site in (A) wild-type -- L212Glu-L213Asp-L225Gly; (B) double mutant -- L212Ala-L213Ala; (C) Class 1 revertant -- L212Ala-L213Asp; (D) Class 2 revertant -- L212Ala-L213Ala-L225Asp. Numbers refer to the *R. capsulatus* sequence (Youvan et al., 1984). The quinone molecule is represented by dashed lines. The double mutant (B) is unable to grow under photosynthetic conditions. The sequence alterations shown in (C) and (D) restore the photosynthetic phenotype. For further discussion of the phenotypes of these strains, see the text.

FIGURE 2: Molecular model, using the *R. sphaeroides* structure, of interactions in (A) the wild-type -- L212Glu-L213Asp-M231Arg; (B) Class 3 revertant -- L212Ala-L213Ala-M231Leu. Numbers refer to the *R. capsulatus*

sequence (Youvan et al., 1984). The quinone molecule is represented by dashed lines. The distant sequence alteration shown (M231Arg → Leu) acts as an intergenic suppressor of the double mutation in the Q_B site, restoring the photosynthetic phenotype.

FIGURE 3: Steady-state photoinduced oxidation of ferrocytochrome c_2 by reaction centers isolated from (A) the wild-type, (B) double mutant, (C) Class 1 revertant, (D) Class 2 suppressor, and (E) Class 3 suppressor strains, recorded at 550 nm in the presence and absence of 300 μM atrazine.

FIGURE 4: Electron transfer kinetics at 770 nm versus 860 nm in wild-type chromatophores following a single laser flash. The kinetics at 860 nm are due to the change in redox states of the bacteriochlorophyll dimer. Kinetics at 770 nm reflect changes in the electrostatic environment of the L-side bacteriopheophytin, which responds to changes in the charged states of Q_A and Q_B, as well as the dimer. An additional fast component is present in the 770 nm kinetics that corresponds to transfer of the charge from Q_A to Q_B.

FIGURE 5: Kinetics of transfer of the first electron from Q_A to Q_B in chromatophores following a single laser flash. When compared to the 860 nm traces, the 770 nm curves contain an additional fast component that is atrazine-sensitive (200 μM). These traces are expansions of the transients recorded in the same manner as that shown in Figure 4. Fits of these curves yielded the lifetimes for the $P^+Q_A^-Q_B \rightarrow P^+Q_AQ_B^-$ reaction

(Table IV). (A) wild-type; (B) double mutant; (C) Class 1 revertant; (D) Class 2 suppressor; (E) Class 3 suppressor.

TABLE I. Amino acids near the quinones.[a]

	Q_B						Q_A				
	[b]vir	sph	cap	rub	aur		vir	sph	cap	rub	aur
L186	A	A	A	A	L	M213	L	L	L	L	L
L189	L	L	M	L	Cys	M216	A	M	M	M	M
L190	His	His	His	His	His	M217	His	His	His	His	His
L193	L	L	L	L	L	M220	Thr	Thr	Thr	Thr	Thr
L194	I	V	V	I	I	M221	I	I	I	I	I
L212	Glu	Glu	Glu	Glu	Glu	M246	A	A	A	A	A
L213	Asn	Asp	Asp	Asn	Asn	M247	A	A	A	A	Gln
L215	Tyr	F	Tyr	Tyr	F	M249	F	F	F	F	F
L216	F	F	F	F	F	M250	W	W	W	W	W
L220	V	V	M	I	Gln	M254	I	M	M	M	M
L222	Tyr	Tyr	Tyr	Tyr	Tyr	M256	F	F	F	F	F
L223	Ser	Ser	Ser	Ser	Ser	M257	Asn	Asn	Asn	Asn	Asn
L224	I	I	V	V	V	M258	A	A	A	A	A
L225	G	G	G	G	G	M259	T	T	T	T	N
L226	A	Thr	Thr	Thr	Glu	M260	I	M	M	M	A
L229	I	I	I	I	V	M263	V	I	I	I	I
L230	His	His	His	His	His	M264	His	His	His	His	His
L232	L	L	L	V	L	M266	W	W	W	W	W
M232	Glu	Glu	Glu	Glu	Glu						

[a]The single-letter code designates hydrophobic amino acids; polar residues are designated with the three-letter code.

[b]vir = *R. viridis*; sph = *R. sphaeroides*; cap = *R. capsulatus*; rub = *R. rubrum*; aur = *C. aurantiacus*.

TABLE II. Revertants and suppressors of the L212-213AA double mutant.

Revertant Strains	Sequence Alterations	Cotransfer of PS^+ with Plasmid	Class
LL4,6	L212Ala remains; L213Ala → Asp	Yes	1
LL1-3 UV7,8 HL1,2,4-7	L212Ala-L213Ala remain; L225Gly → Asp	Yes	2
LL7,8	L212Ala-L213Ala remain; M231Arg → Leu	Yes	3
HL8	L212Ala-L213Ala remain; no mutations found in sequenced regions[a]	Yes	4[b]
UV1-6 LL5 HL3	L212Ala-L213Ala remain; no mutations found in sequenced regions	No	5[b]

[a]Sequenced regions - *pufL, pufM.*

[b]Class 4 and Class 5 suppressor apparently do not reside in the L or M chains. These strains are subject to ongoing study.

TABLE III. P^+Q^- → PQ charge recombination kinetics, measured at 810 nm in LDAO-treated chromatophores after a single laser flash.

	- atrazine				+ atrazine			
	fast phase		slow phase		fast phase		slow phase	
	τ_F (ms)	%	τ_S (ms)	%	τ_F (ms)	%	τ_S (ms)	%
Wild-type	60	40	700	60	40	75	200	25
Double mutant	40	67	300	33	30	63	200	37
Class 1 revertant	75	30	300	70	50	75	300	25
Class 2 suppressor	60	34	300	66	50	49	300	51
Class 3 suppressor	50	25	900	75	35	77	400	23

TABLE IV. Kinetics of $Q_A^- Q_B \rightarrow Q_A Q_B^-$ electron transfer in chromatophores, obtained from the fast decay component in the 770 nm transients.

	- atrazine		+ atrazine	
	$\tau(\mu s)$	%	$\tau(\mu s)$	%
Wild-type	55 (± 15)	17	76 (± 12)	5
Double mutant	80 (± 10)	4	89 (± 1)	3
Class 1 revertant	84 (± 4)	16	100 (± 20)	
Class 2 suppressor	137 (± 4)	14	123 (± 10)	10
Class 3 suppressor	48 (± 14)	9	73 (± 10)	4

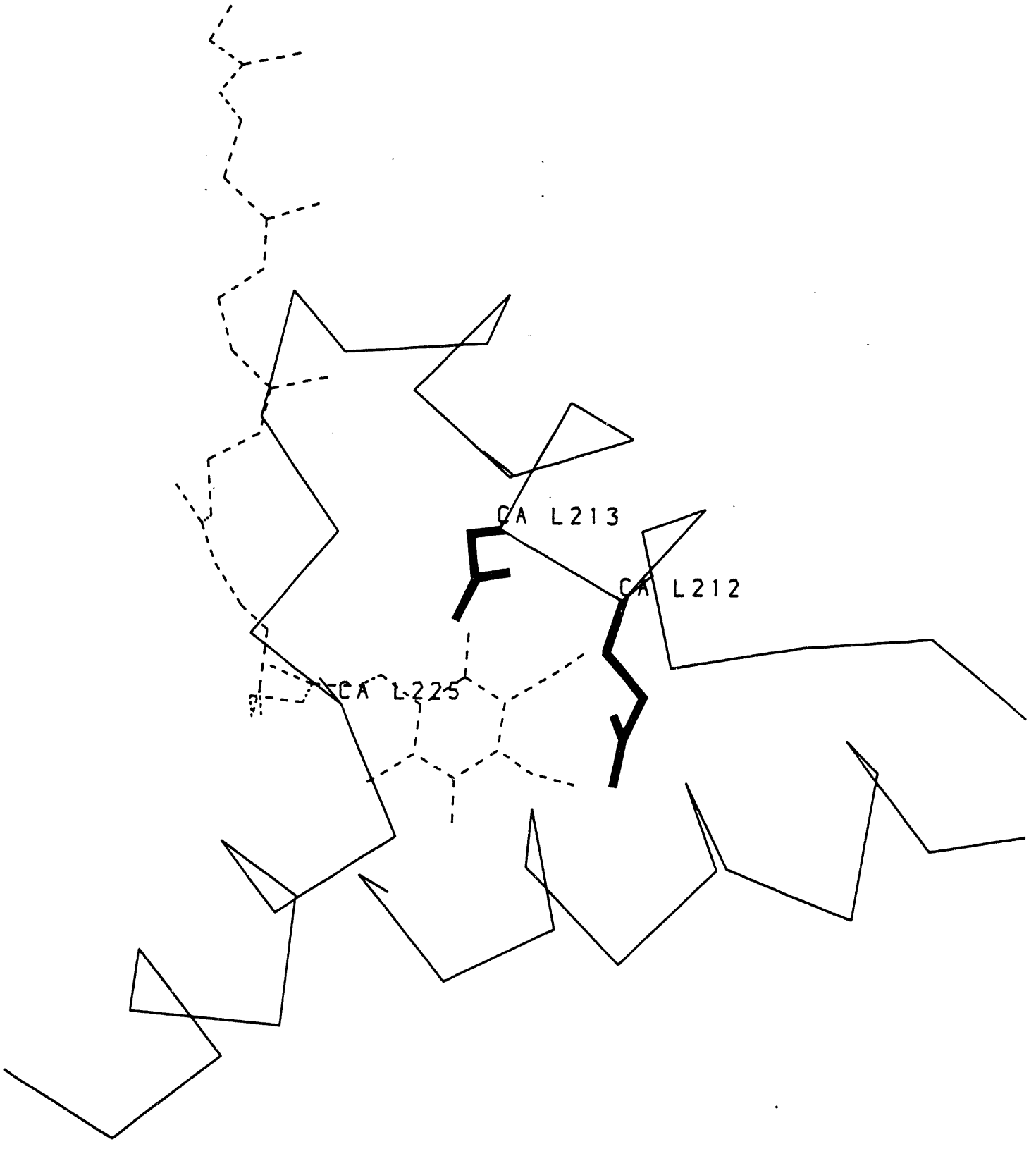
CA L213
CA L212
CA L225

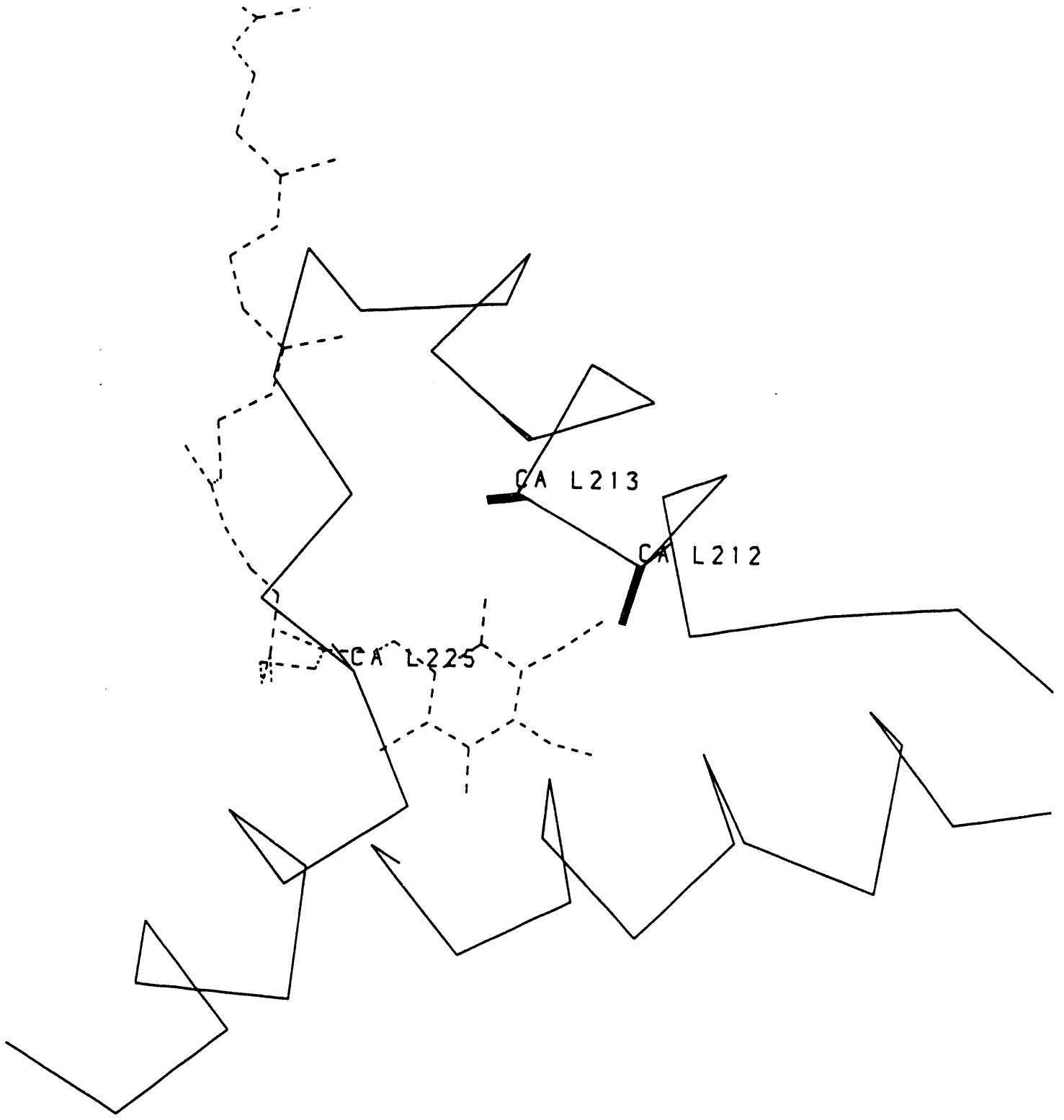
CA L213
CA L212
CA L225

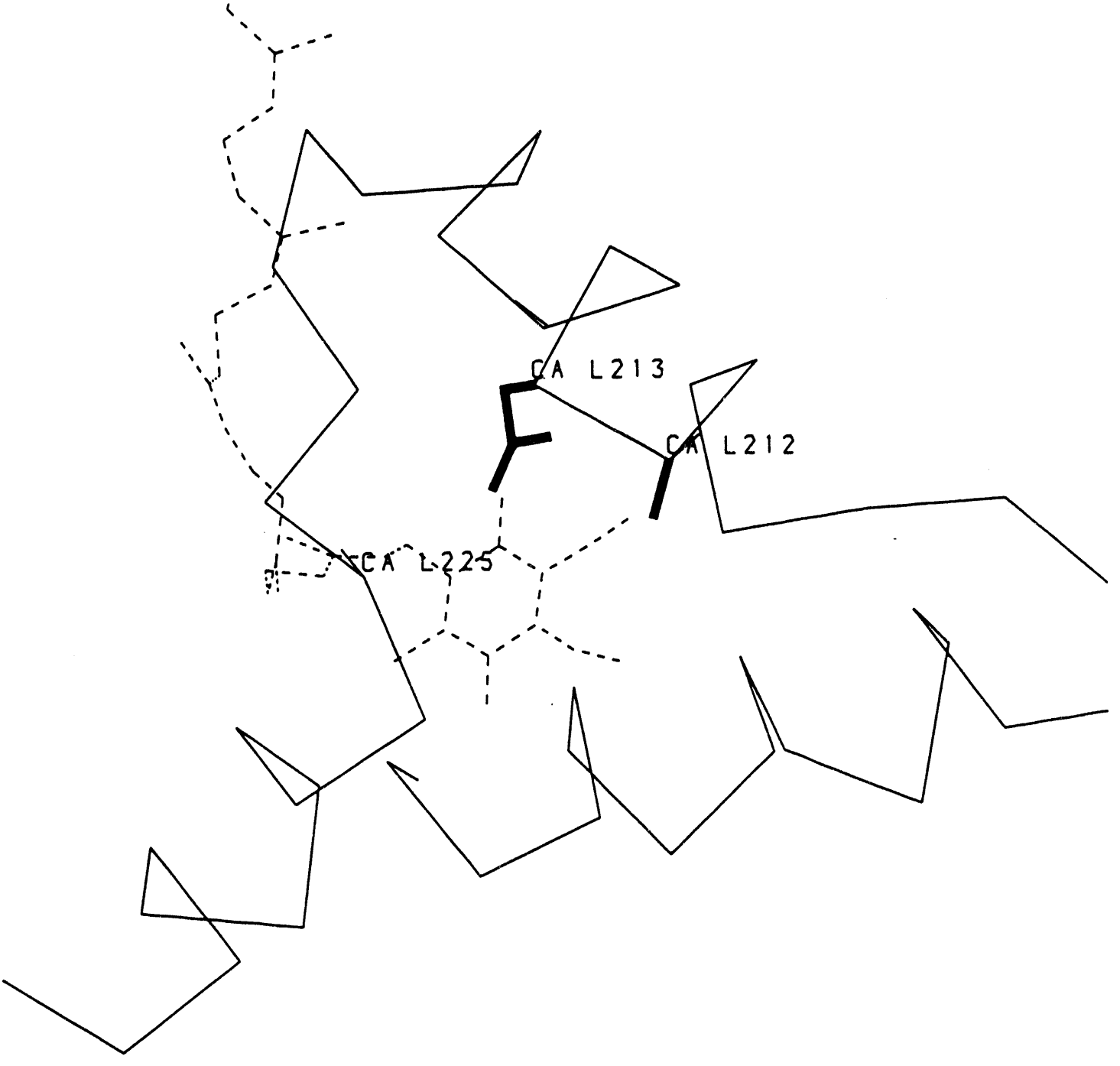
CA L213
CA L212
CA L225

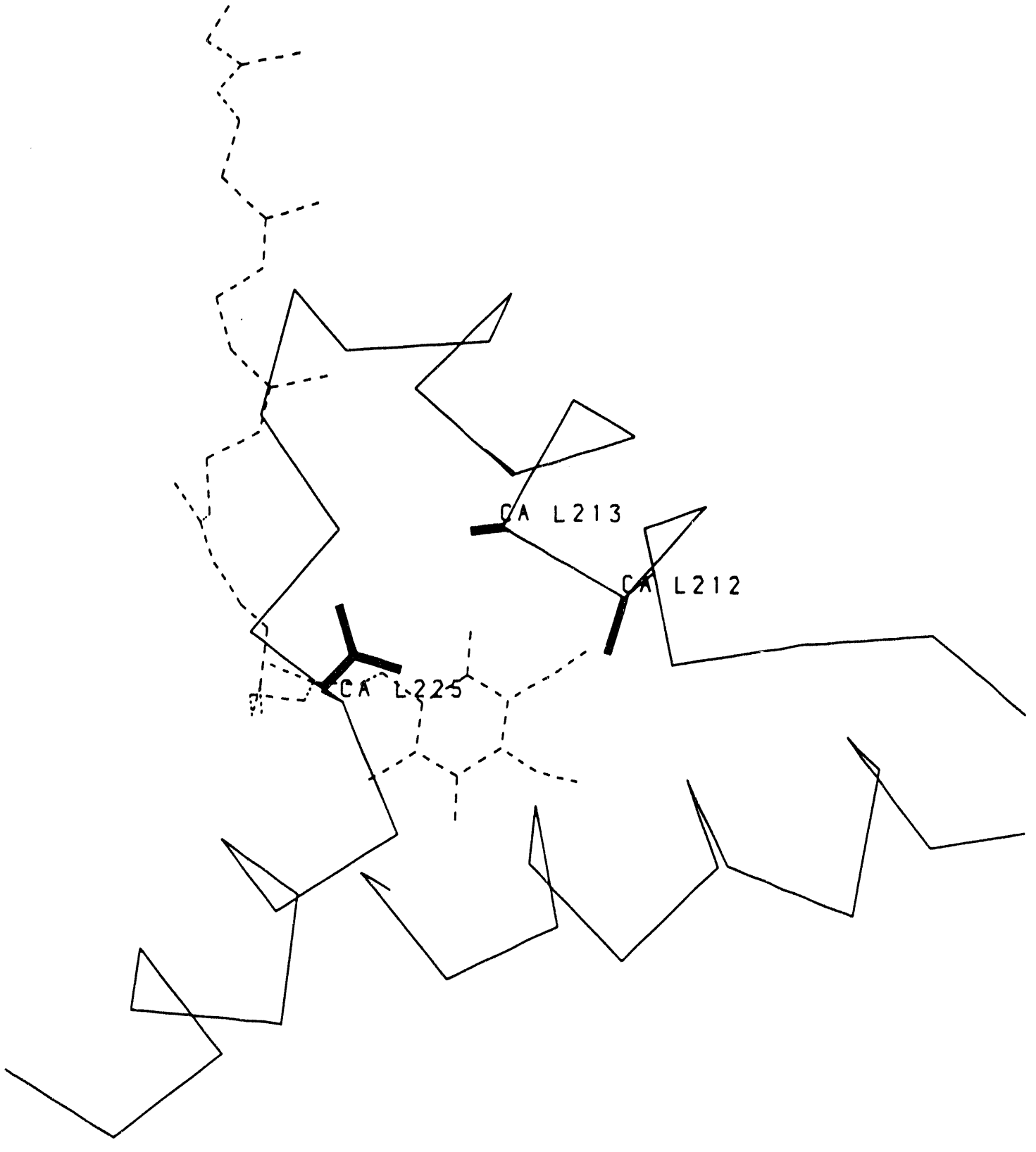

Figure 1d

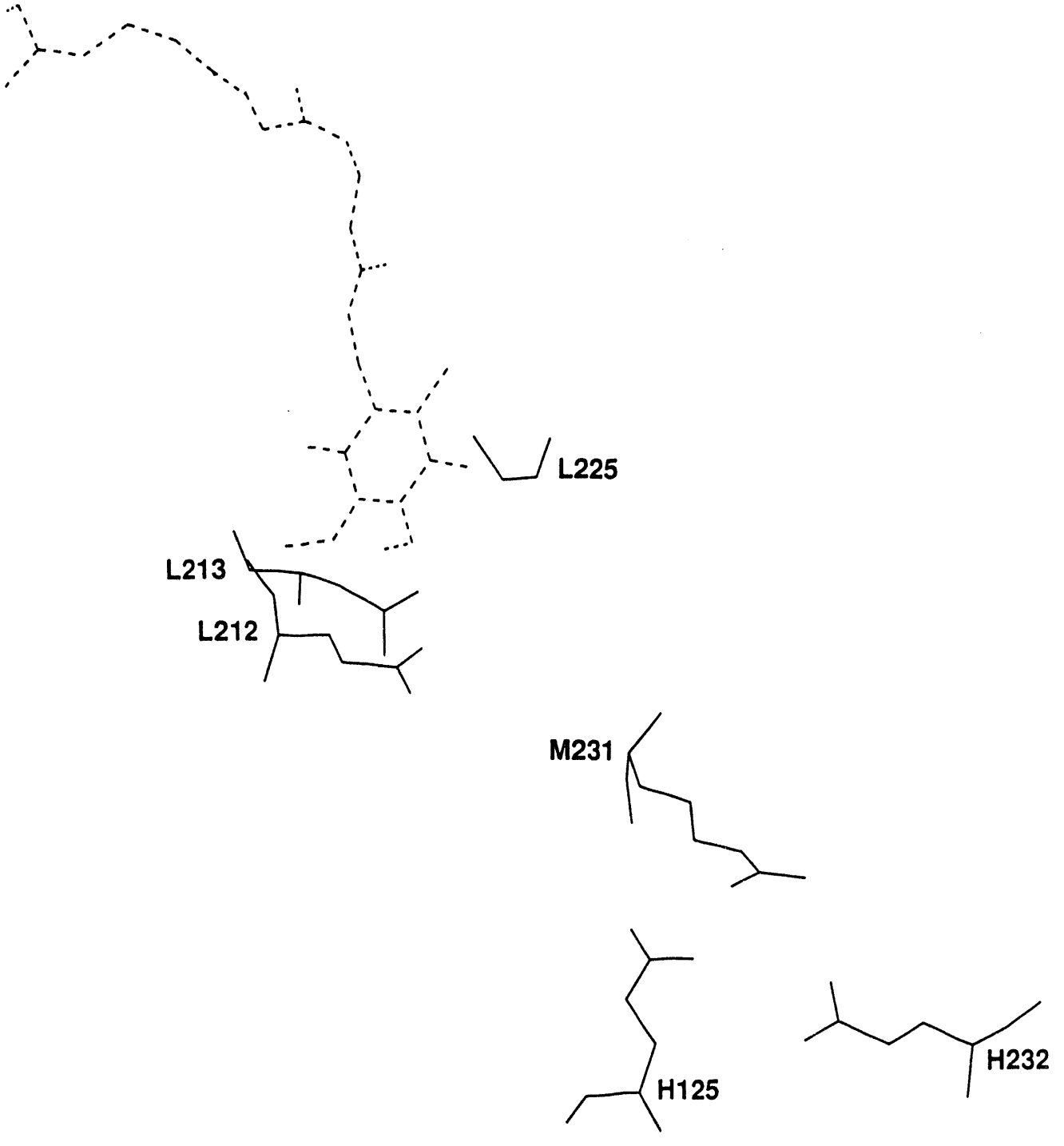

Figure 2

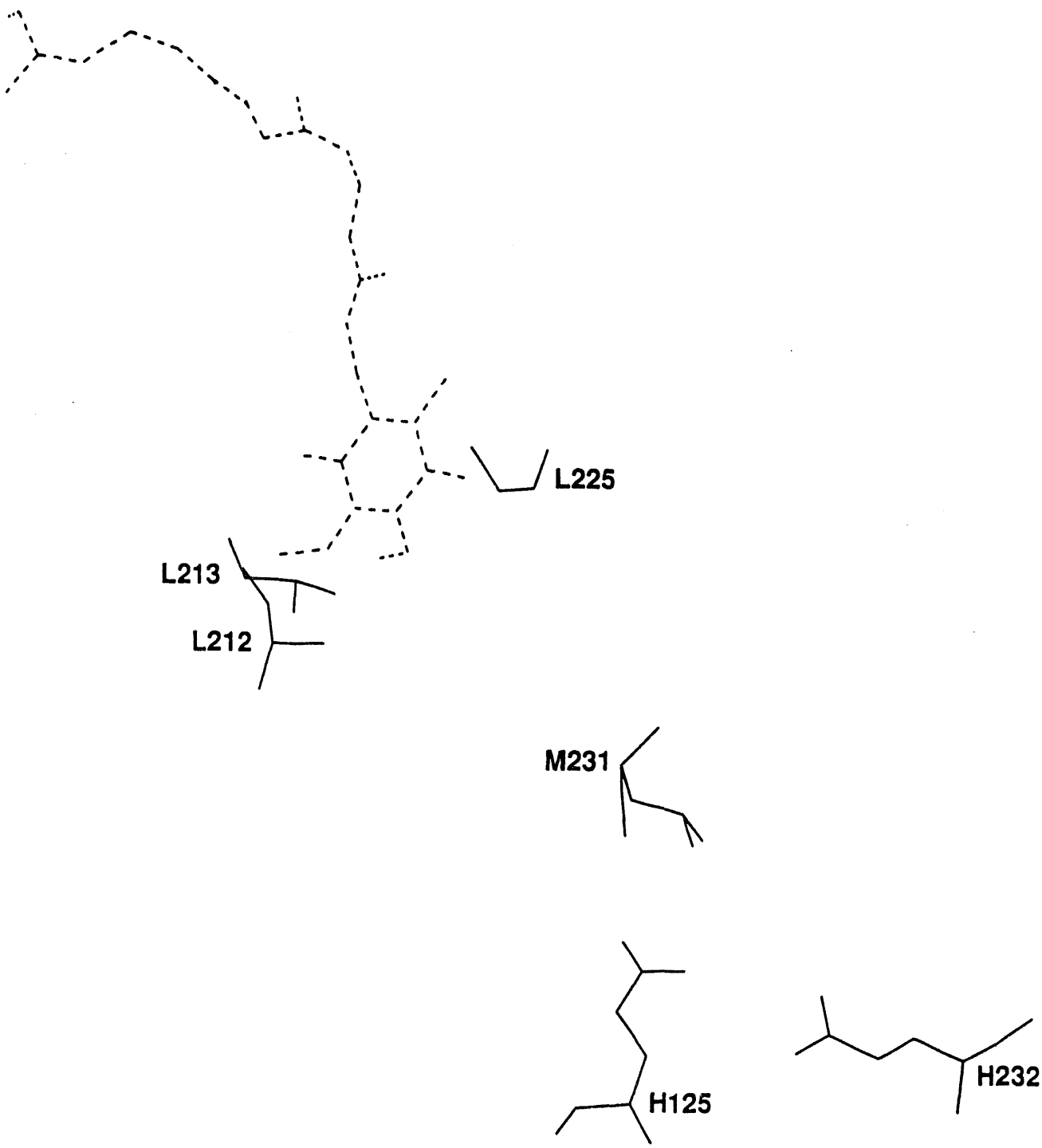

Figure 2b

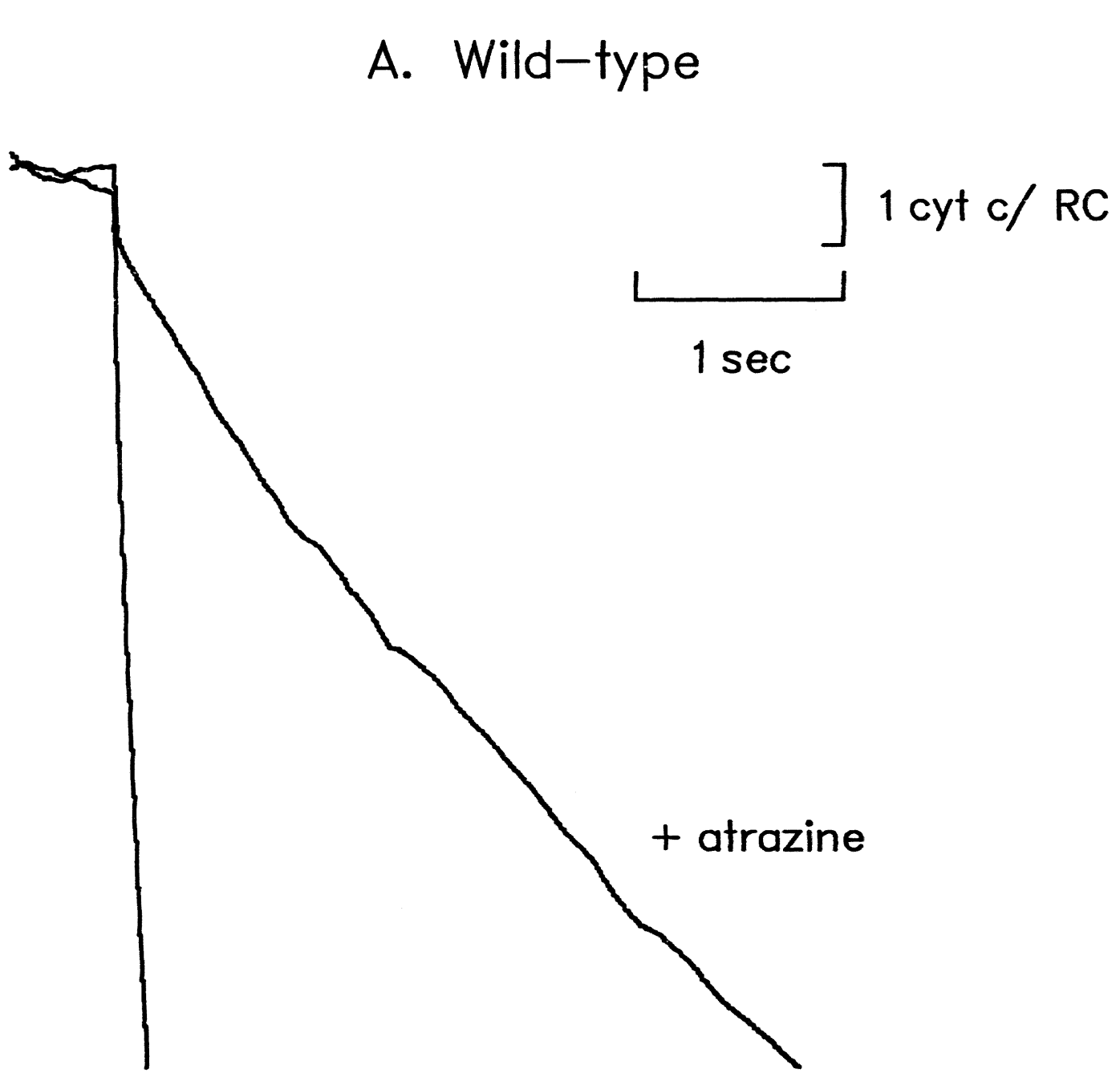
A. Wild–type
1 cyt c/ RC
1 sec
+ atrazine

B. Double Mutant

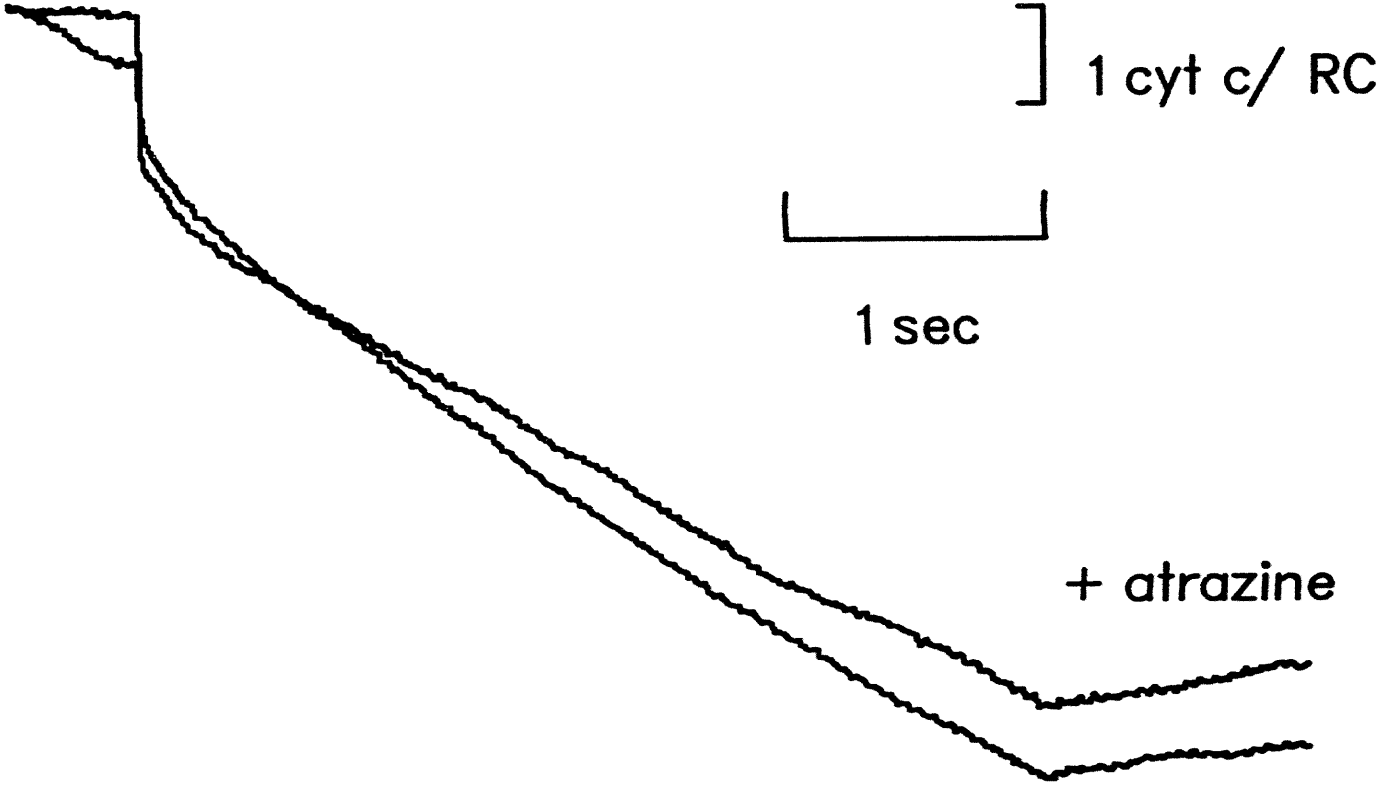

C. Class 1 Revertant

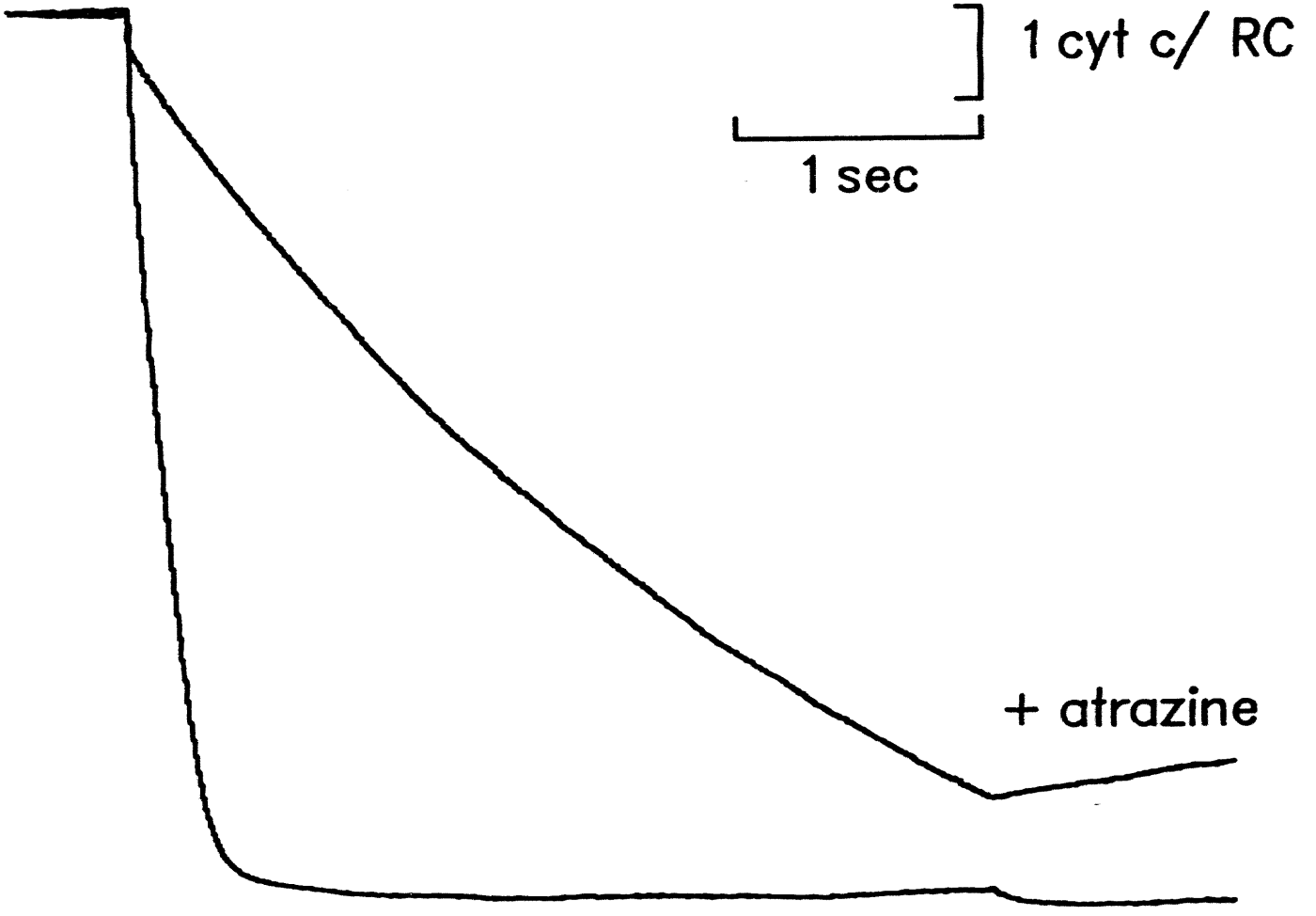

D. Class 2 Suppressor

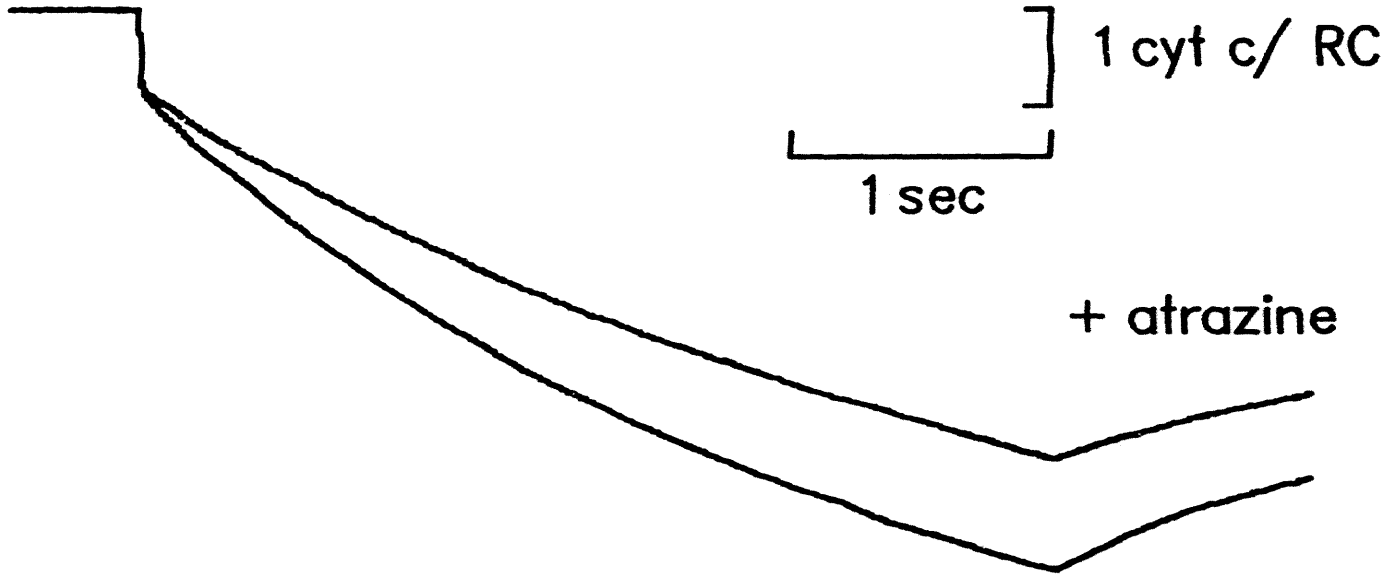

E. Class 3 Suppressor

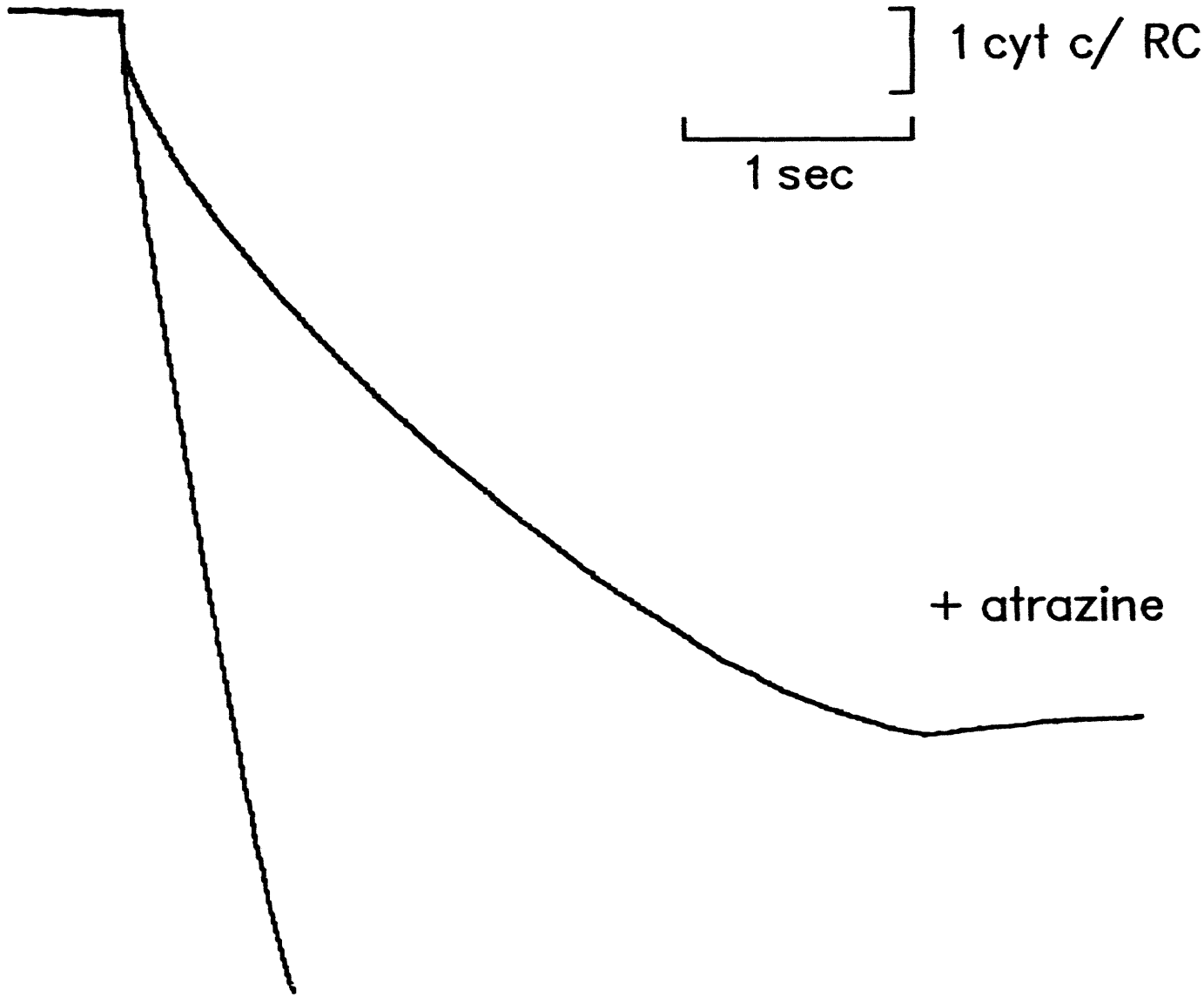

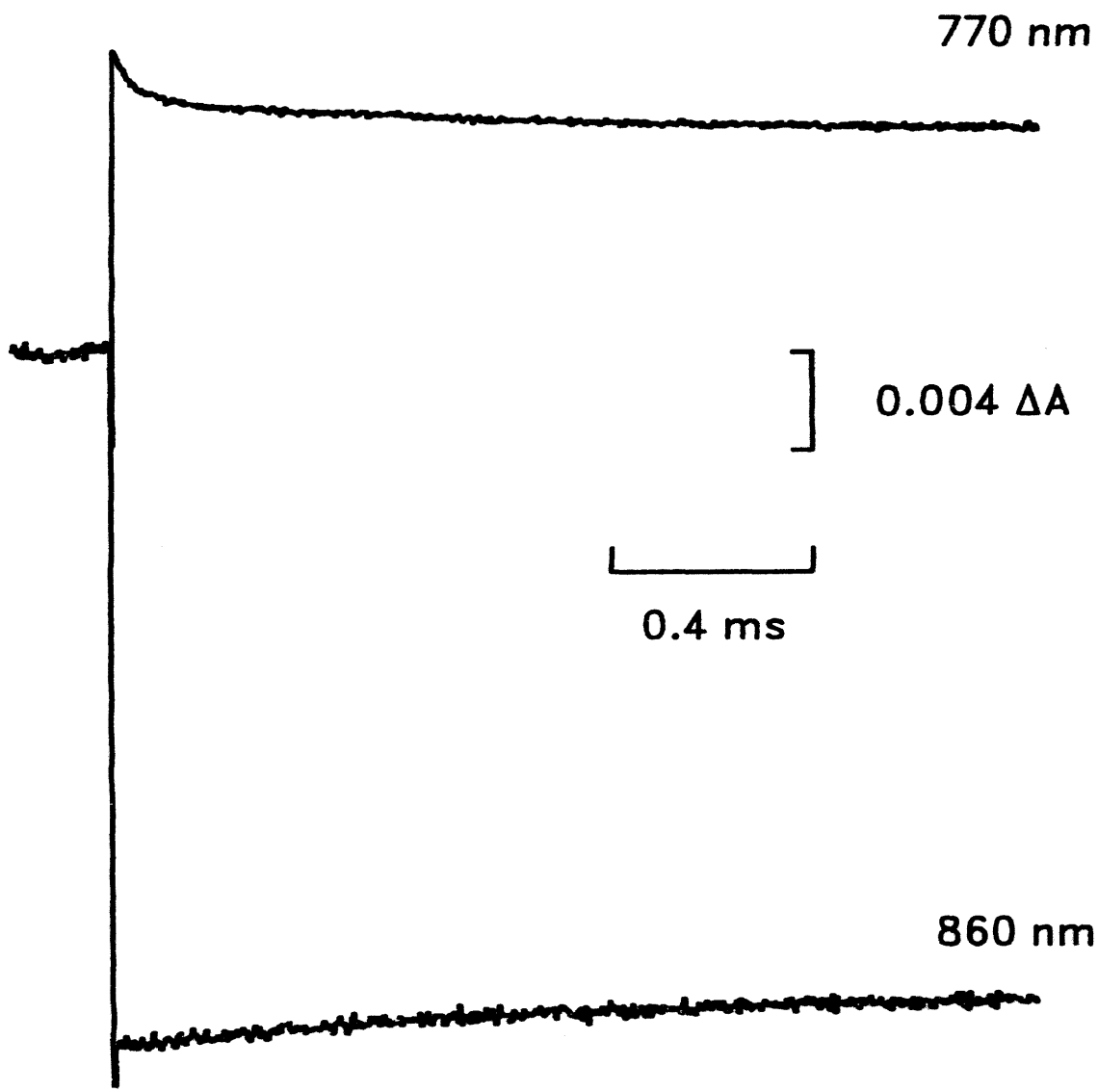
770 nm
0.004 ΔA
0.4 ms
860 nm

A. Wild–type

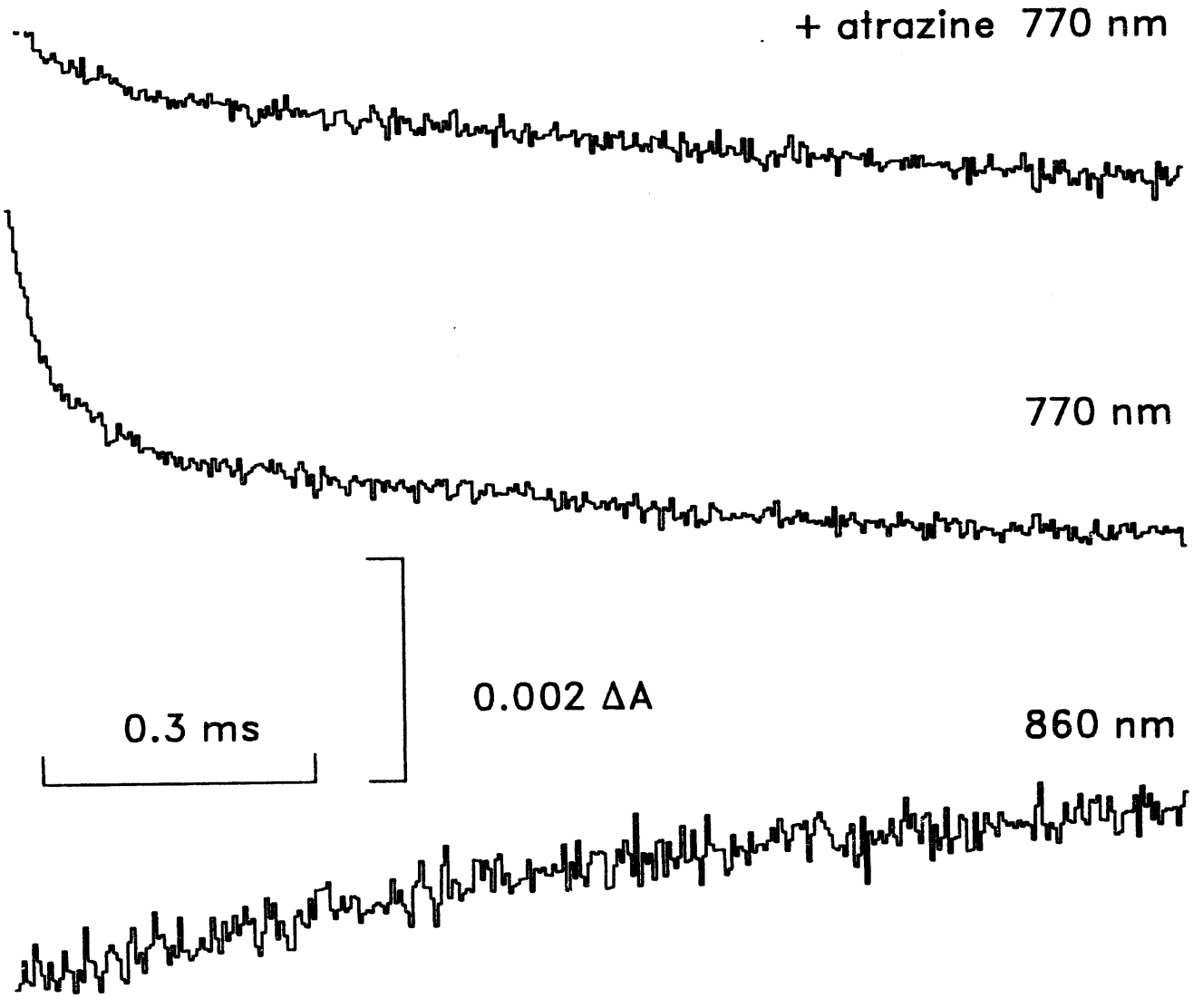

B. Double Mutant

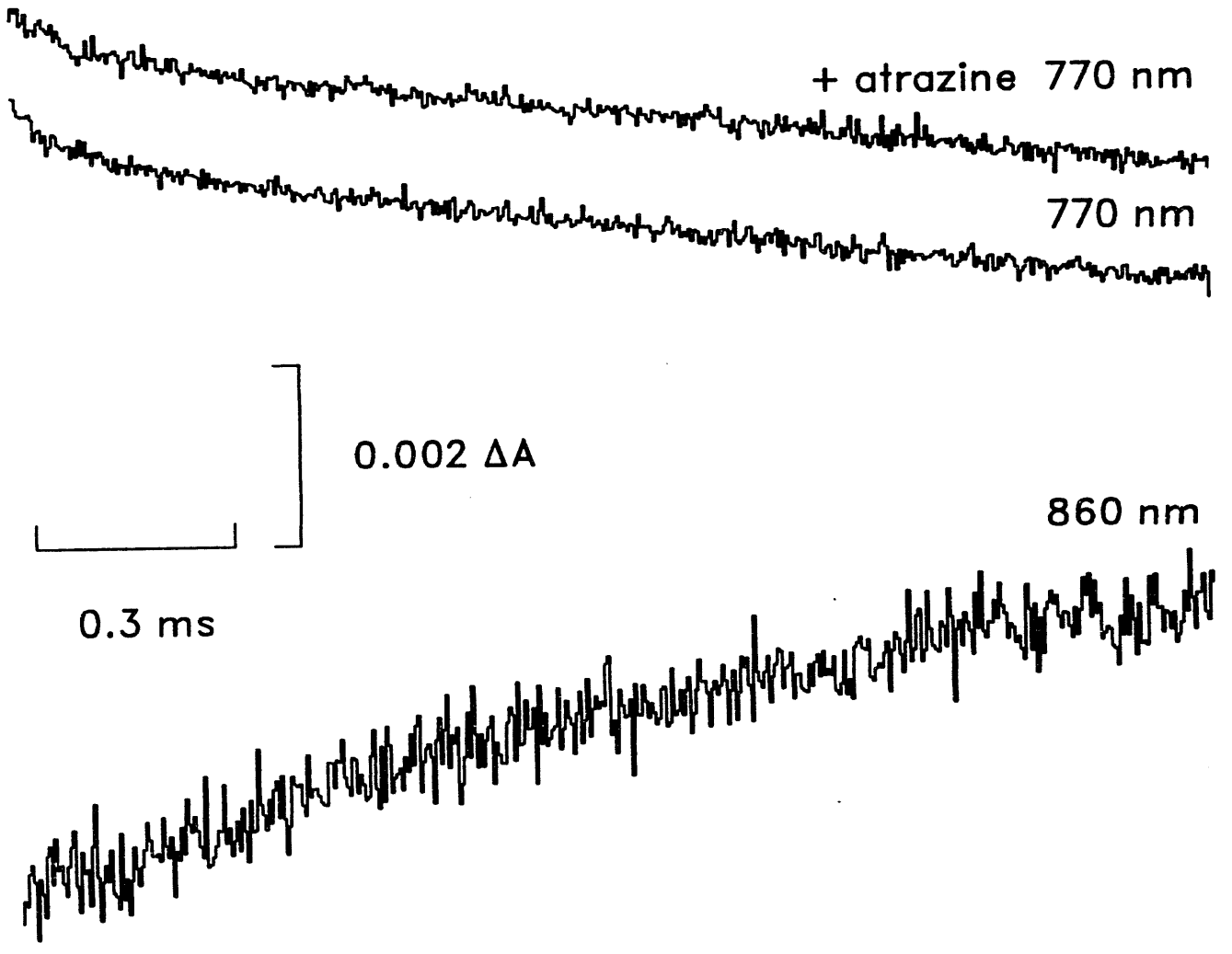

C. Class 1 Revertant

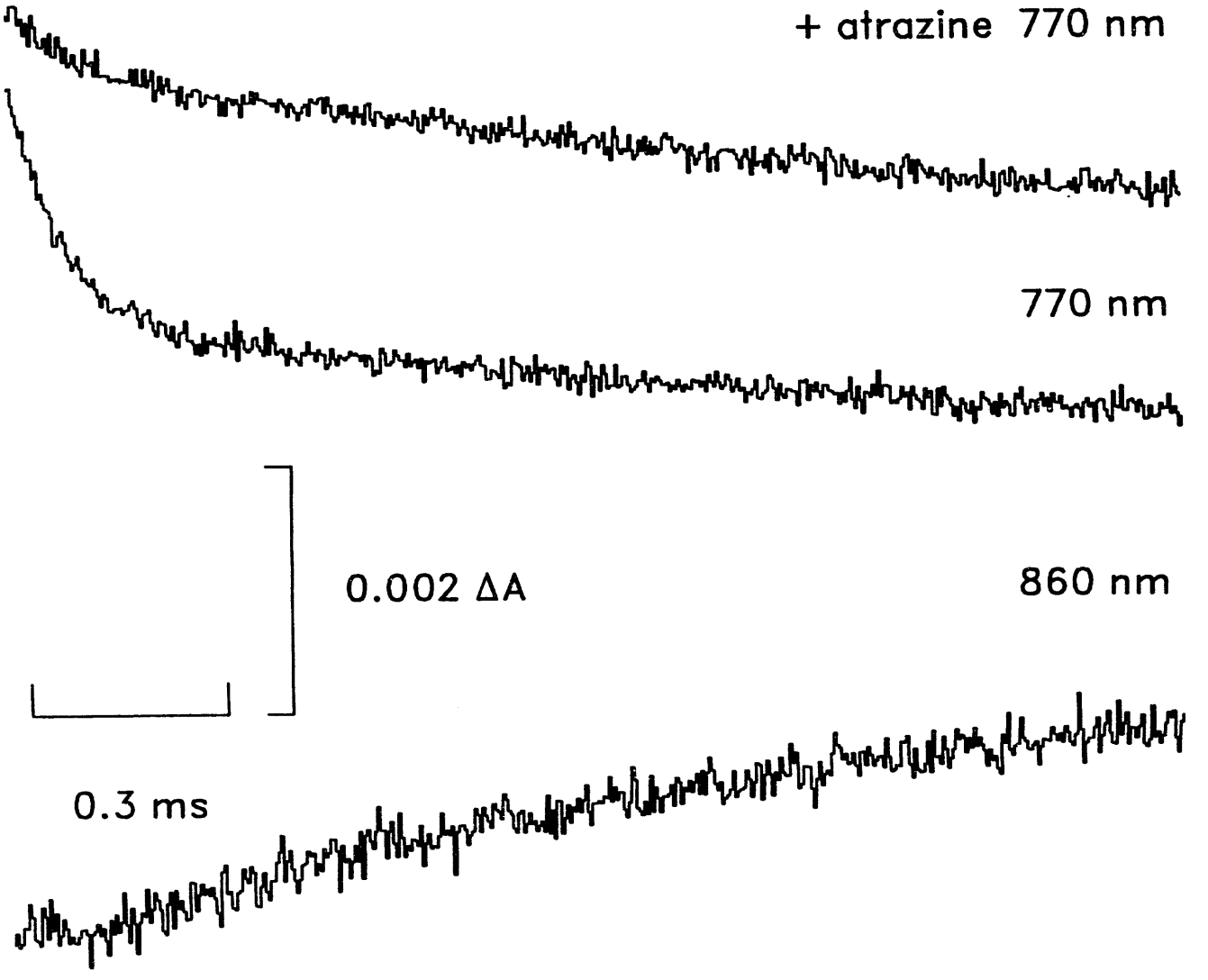

D. Class 2 Suppressor

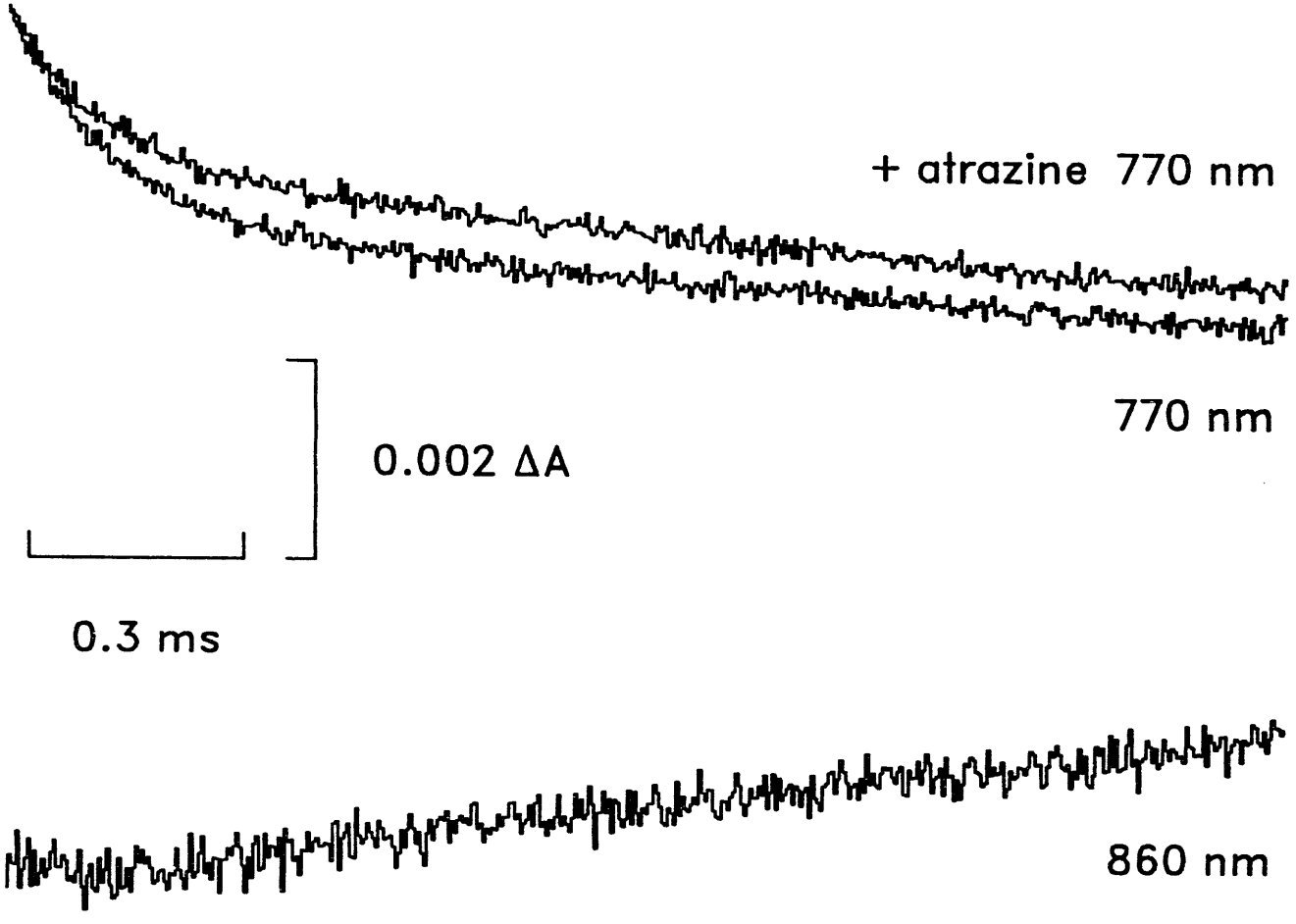

E. Class 3 Suppressor

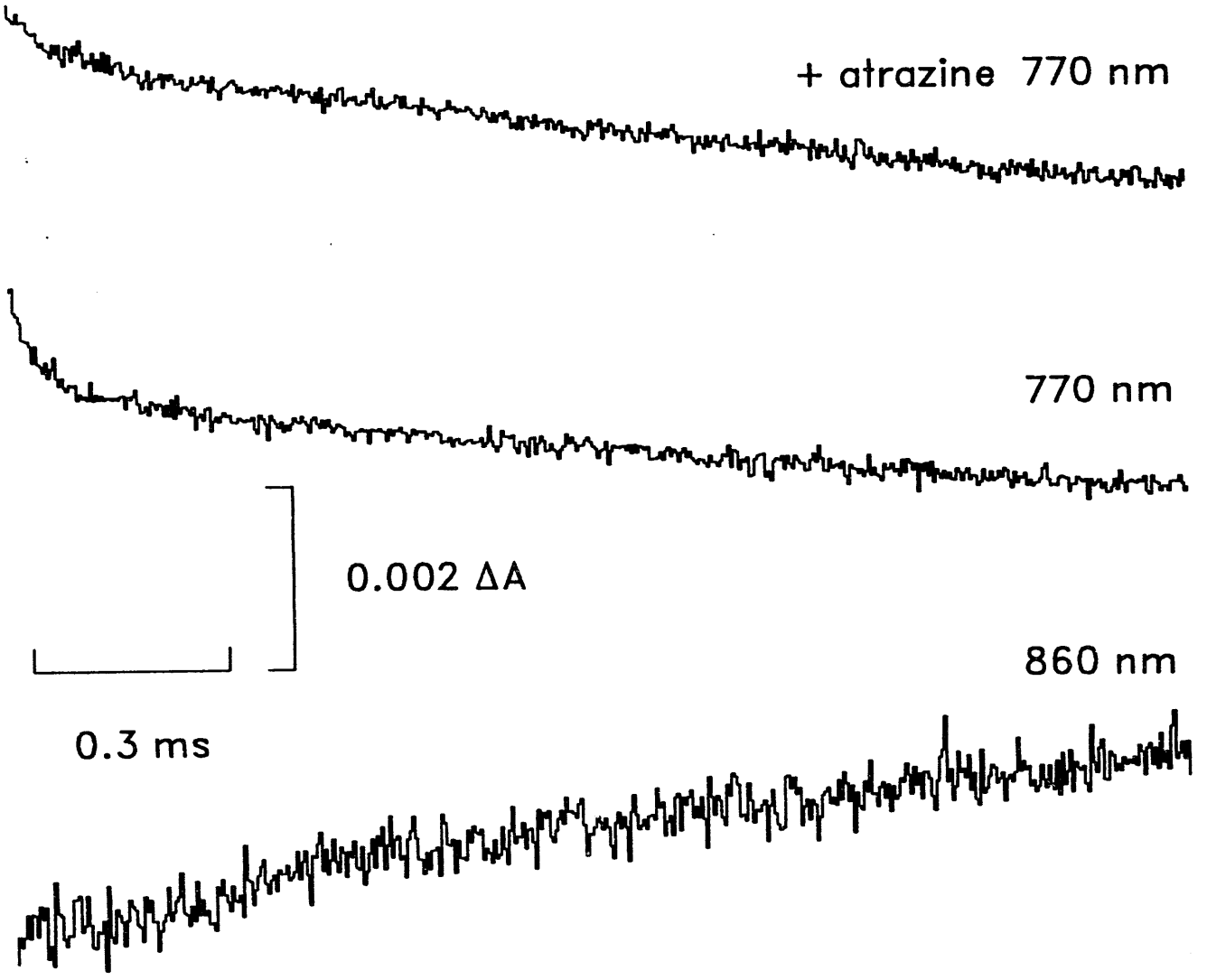

DATE
FILMED
6/14/94
END